AD-780 776

HYDROELASTIC DESIGN OF SUBCAVITATING AND CAVITATING HYDROFOIL STRUT SYSTEMS

Peter K. Besch, et al

Naval Ship Research and Development Center
Bethesda, Maryland
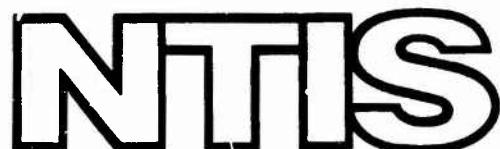
April 1974

MAJOR NSRDC ORGANIZATIONAL COMPONENTS

*REPORT ORIGINATOR

NSRDC
COMMANDER 00
TECHNICAL DIRECTOR 01

OFFICER-IN-CHARGE
CARDEROCK 05

OFFICER-IN-CHARGE
ANNAPOLIS 04

SYSTEMS
DEVELOPMENT
DEPARTMENT 11

SHIP PERFORMANCE
DEPARTMENT 15

AVIATION AND
SURFACE EFFECTS
DEPARTMENT 16

STRUCTURES
DEPARTMENT 17

COMPUTATION
AND MATHEMATICS
DEPARTMENT 18

SHIP ACOUSTICS
DEPARTMENT 19

PROPULSION AND
AUXILIARY SYSTEMS
DEPARTMENT 27

MATERIALS
DEPARTMENT 28

CENTRAL
INSTRUMENTATION
DEPARTMENT 29
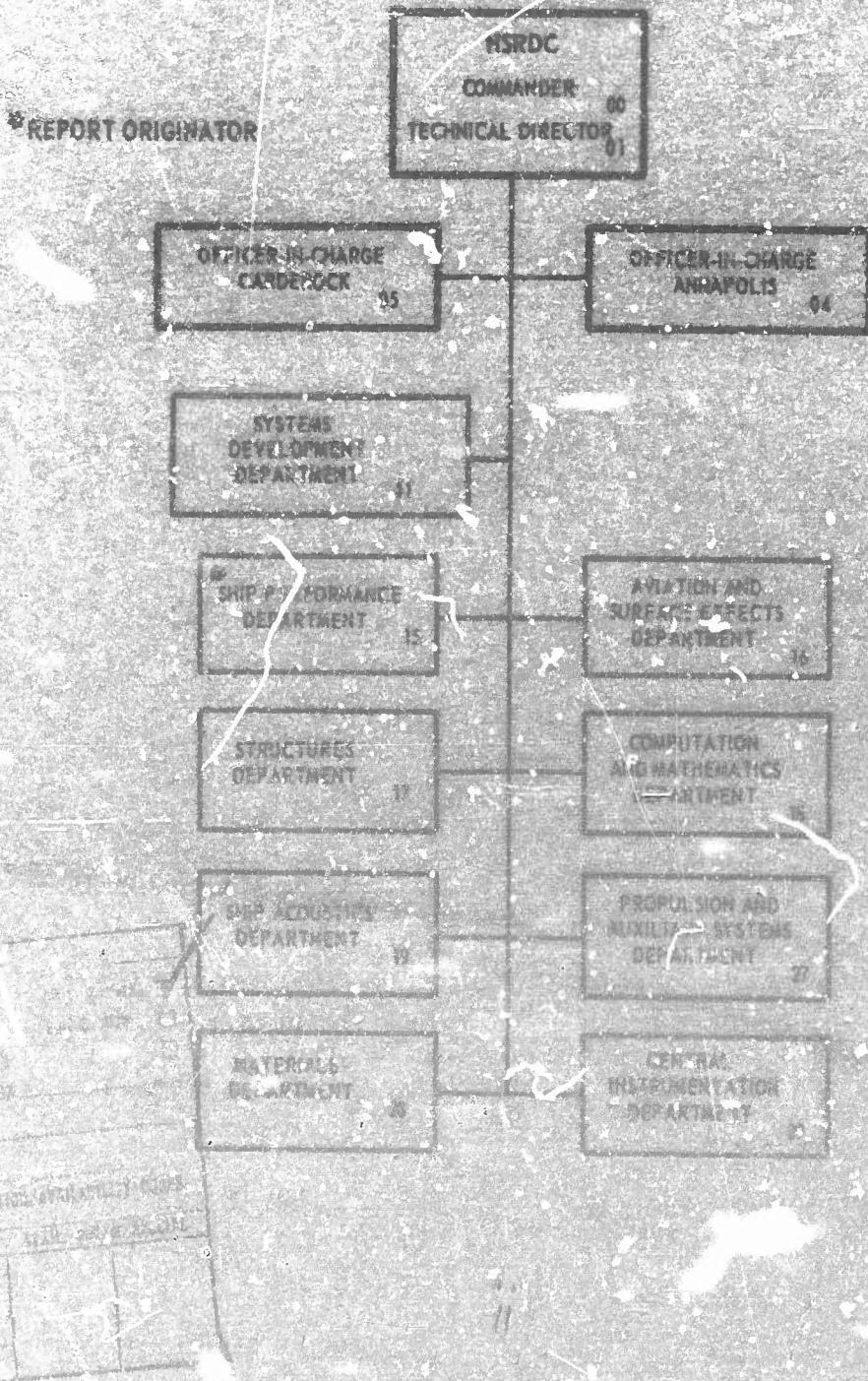
AD- 780776

REPORT DOCUMENTATION PAGE	READ INSTRUCTIONS BEFORE COMPLETING FORM

1. REPORT NUMBER	2. GOVT ACCESSION NO.	3. RECIPIENT'S CATALOG NUMBER
4257		

4. TITLE (and Subtitle)	5. TYPE OF REPORT & PERIOD COVERED
HYDROELASTIC DESIGN OF SUBCAVITATING AND CAVITATING HYDROFOIL STRUT SYSTEMS	
	6. PERFORMING ORG. REPORT NUMBER

7. AUTHOR(s)	8. CONTRACT OR GRANT NUMBER(s)
Peter K. Besch and Yuan-Ning Liu	

9. PERFORMING ORGANIZATION NAME AND ADDRESS	10. PROGRAM ELEMENT, PROJECT, TASK AREA & WORK UNIT NUMBERS
Naval Ship Research and Development Center Bethesda, Maryland 20034	NAVSHIPS Subproject S4606, Task 1703, Work Unit 1153-003 and NAVMAT Program Element o2754N, Task Area ZF43421001 Work Unit 1520-001

11. CONTROLLING OFFICE NAME AND ADDRESS	12. REPORT DATE
	April 1974
	13. NUMBER OF PAGES
	85

14. MONITORING AGENCY NAME & ADDRESS(if different from Controlling Office)	15. SECURITY CLASS. (of this report)
Naval Ship Systems Command Naval Material Command	UNCLASSIFIED
	15a. DECLASSIFICATION/DOWNGRADING SCHEDULE

16. DISTRIBUTION STATEMENT (of this Report)

APPROVED FOR PUBLIC RELEASE: DISTRIBUTION UNLIMITED

17. DISTRIBUTION STATEMENT (of the abstract entered in Block 20, if different from Report)

18. SUPPLEMENTARY NOTES

19. KEY WORDS (Continue on reverse side if necessary and identify by block number)

Hydrofoil—Flutter—Bending, Torsional—Divergence, Strut

Vibration—Flutter—Bending, Torsional — Design—Hydroelastic—Flutter, Divergence—Strut

Model—Hydroelastic, Scaling, AGEH

20. ABSTRACT (Continue on reverse side if necessary and identify by block number)

This report presents design procedures and parametric trends that can be used to avoid flutter and divergence of hydrofoil strut-foil systems. Flutter stability of conventional T-foils can be achieved by scaling existing prototype systems which are stable; scaled flutter models must be used to determine the stability of new designs. Several stable T-foil designs are available for craft with displacements of up to 300 tons at subcavitating speeds (below 50 knots).

(Continued on back)

DD FORM 1473 EDITION OF 1 NOV 65 IS OBSOLETE
1 JAN 73
S/N 0102-014-6601

20. The availability of higher speed designs for ships of practical size is limited to one system that is stable to 62 knots. Divergence stability of subcavitating systems can be ensured by theoretical analysis using an available computer program.

ia

TABLE OF CONTENTS

iii

LIST OF FIGURES

NOTATION

AR	Aspect ratio of submerged structure; (submerged span)^2/ (submerged area)
c	Chord length of strut, measured perpendicular to elastic axis
c_{root}	Chord length of foil extended to pod centerline, measured parallel to free stream
c_s	Structural damping of a given vibration mode
EI	Bending stiffness of section normal to elastic axis
F_n	Froude number based on streamwise chord of strut; $U/\sqrt{gc/\cos \Lambda}$
f	Frequency of oscillation
f_f	Frequency of oscillation at flutter inception
GJ	Torsional stiffness of section normal to elastic axis
g	Acceleration due to gravity
H	Amplitude of bending displacement
h	Local depth at elastic axis
I_{my}	Moment of inertia per unit span of strut, in air, about strut elastic axis
$I_{mz'}$	Moment of inertia per unit span of foil, in air, about foil elastic axis
I_y	Total moment of inertia of strut, pod, or foil, in air, about strut elastic axis
I_y*	Total added moment of inertia of strut, pod, or foil due to rotation about strut elastic axis
I_ϕ	Total moment of inertia of structure, in air, about pod centerline
k_{nf}	Reduced frequency at flutter inception; $c\omega_f/2U_{nf}$
L	Length of strut or foil along elastic axis
ℓ	Submerged length of strut elastic axis
M	Total mass of structure, in air
M*	Total added mass of strut or pod due to translation normal to strut chord plane
m	Mass per unit span, in air
p_a	Pressure of atmosphere above free surface
p_c	Pressure in a cavity
U	Flow speed, or speed of structure through fluid
U_D	Flow speed at divergence instability
U_f	Flow speed at flutter inception
U_{nf}	Component of flow velocity at flutter inception, normal to strut elastic axis; $U_f \cos \Lambda$

x_{cg}	Distance from strut leading edge to local strut center of gravity, measured perpendicular to strut elastic axis
x_{ea}	Distance from strut leading edge to local strut elastic axis location, measured perpendicular to elastic axis
x_{foil}	Distance from leading edge of foil to leading edge of strut, measured along pod centerline, positive aft
x_{nose}	Distance from pod nose to leading edge of strut, measured along centerline of pod
y	Spanwise coordinate along strut elastic axis
z'	Spanwise coordinate along foil elastic axis
ζ(zeta)	Damping ratio; damping as a fraction of critical damping
ζ_s	Damping ratio due to structural damping
ζ'	Normalized spanwise location on foil; z'/L_{foil}
η(eta)	Normalized spanwise location on strut; y/L_{strut}
θ(theta)	Amplitude of torsional displacement
κ(kappa)	Sweep parameter; $(c \tan \Lambda)/L$
Λ(lambda)	Sweep angle of quarter chord, positive for sweepback
μ(mu)	Generalized mass ratio
$\mu_{bending}$	Approximation to generalized mass ratio for bending motion
$\mu_{torsion}$	Approximation to generalized mass ratio for torsional motion
π(pi)	$\simeq 3.1416$
ρ(rho)	Mass density of fluid in which structure is operated
σ(sigma)	Cavitation number based on water vapor pressure
σ_c	Cavitation number based on actual cavity pressure
τ(tau)	Taper ratio; (foil tip chord)/(foil root chord)
ω(omega)	Circular frequency of oscillation; $2\pi f$
ω_α	Circular frequency of first torsional vibration mode in air

Subscripts

foil	Value associated with foil
model	Value associated with model system, usually much smaller than full scale
N	Value normalized with respect to value at some spanwise position
pod	Value associated with pod
prototype	Value associated with prototype system, usually a full-scale system
strut	Value associated with strut

ix

ABSTRACT

This report presents design procedures and parametric tre.:ds that can be used to avoid flutter and divergence of hydrofoil strut-foil systems. Flutter stability of conventional T-foils can be achieved by scaling existing prototype systems which are stable; scaled flutter models must be used to determine the stability of :i w designs. Several stable T-foil designs are available for craft with displacements of up to 300 tons at subcavitating speeds (below 50 knots). The availability of higher speed designs for ships of practical size is limited to one system that is stable to 62 knots. Divergence stability of subcavitating systems can be ensured by theoretical analysis using an available computer program.

ADMINISTRATIVE INFORMATION

INTRODUCTION

In this report, results of flutter and divergence research have been rephrased for practical application by the designer. Procedures are included both for producing a preliminary design and for evaluating a final design.

The appendages of high-speed ships must be free of hydroelastic instability (flutter and divergence). To date, all such appendages have been free of these problems. Divergence stability was achieved by using calculations that were sufficiently accurate for design purposes. However, because flutter boundaries could not be calculated accurately, other design criteria were responsible for the flutter stability of existing struts and foils. These were based on maximum expected stress levels. Specifically, struts and foils suitable for use in rough seas were rigid enough to resist flutter and divergence. Despite the proven stability of existing designs, hydroelastic prediction techniques are needed for reassurance on the stability of future conventional appendage designs as well as for the successful design of unconventional appendages.

Notwithstanding recent significant advances in understanding flutter and divergence, neither existing data nor theoretical analyses are presently adequate to offer accurate predictions of flutter boundaries. Therefore, the designer of future systems is offered only an

1

ABSTRACT

This report presents design procedures and parametric trends that can be used to avoid flutter and divergence of hydrofoil strut-foil systems. Flutter stability of conventional T-foils can be achieved by scaling existing prototype systems which are stable; scaled flutter models must be used to determine the stability of new designs. Several stable T-foil designs are available for craft with displacements of up to 300 tons at subcavitating speeds (below 50 knots). The availability of higher speed designs for ships of practical size is limited to one system that is stable to 62 knots. Divergence stability of subcavitating systems can be ensured by theoretical analysis using an available computer program.

ADMINISTRATIVE INFORMATION

INTRODUCTION

In this report, results of flutter and divergence research have been rephrased for practical application by the designer. Procedures are included both for producing a preliminary design and for evaluating a final design.

The appendages of high-speed ships must be free of hydroelastic instability (flutter and divergence). To date, all such appendages have been free of these problems. Divergence stability was achieved by using calculations that were sufficiently accurate for design purposes. However, because flutter boundaries could not be calculated accurately, other design criteria were responsible for the flutter stability of existing struts and foils. These were based on maximum expected stress levels. Specifically, struts and foils suitable for use in rough seas were rigid enough to resist flutter and divergence. Despite the proven stability of existing designs, hydroelastic prediction techniques are needed for reassurance on the stability of future conventional appendage designs as well as for the successful design of unconventional appendages.

Notwithstanding recent significant advances in understanding flutter and divergence, neither existing data nor theoretical analyses are presently adequate to offer accurate predictions of flutter boundaries. Therefore, the designer of future systems is offered only an

1

indirect approach, utilizing either the performance of existing full-scale hydrofoil structures or simulation with scaled flutter models. Quantitative stability boundaries can be established on the basis of the general scaling laws provided.

The present report gives a method of theoretical analysis which is sufficiently accurate for divergence prediction and, in some cases, flutter prediction also. Subcavitating and cavitating systems are treated separately. The report includes a brief description of flap reversal, a hydroelastic effect which nullifies the control effect of a flap and therefore must be avoided. It is not an instability, however. A typical inverted-T strut-pod-foil system is shown in Figure 1. Most available research, however, deals with struts without foils. On hydrofoil craft, T-foils appear to be relatively more vulnerable to hydroelastic instability than do inverted-pi foils, the other common configuration. Inverted-pi foils are more stable because the struts and inboard foil sections are multiply constrained.

DESCRIPTION OF FLUTTER, DIVERGENCE, AND FLAP REVERSAL

FLUTTER

Flutter is the unstable oscillation of a structure composed of lifting surfaces traveling through a fluid. The oscillation increases exponentially in amplitude until the structure yields or the flow changes in some way. The strut-foil systems on hydrofoil craft and the strut-like rudders expected to be used on surface effect ships are examples of structures which may be vulnerable to flutter.

Flutter characteristics of structures are specified in terms of speed boundaries which separate regions of positive and negative damping. The boundaries are composed of critical flutter speeds, also known as flutter inception speeds, and correspond to zero damping of the system. At a critical flutter speed, an oscillation triggered by a deflection of the structure will continue at constant amplitude. Above this speed, an oscillation will increase in amplitude. It is expected that there will be sufficient unsteadiness in water flow to trigger oscillation at or above the flutter speed.

Bending and Torsional Flutter Modes

Experimental and theoretical results indicate that cantilevered struts undergo flutter in two different hydroelastic modes. Based on the predominant structural mode shapes

Figure 1 – 1/8-Scale Flutter Model of Main T-Foil System for
AGEH (PLAINVIEW)

3

involved these modes have been designated as bending flutter and torsional flutter.[1] Since the flutter characteristics of each mode are significantly different, it is important to identify the mode to be expected for a given strut.

The flutter mode of a strut can be determined by examining the mode shape of its second vibration mode in water, except in a transition region where strong coupling of structural modes occurs. Mode shapes are designated by their similarity to the uncoupled mode shapes of a cantilever beam, which are shown in Figure 2. All struts exhibit a fundamental (lowest frequency) vibration mode shape that resembles first bending. However, the marked difference exhibited by struts in their second (next-to-lowest frequency) mode shapes permits identification of the flutter mode. If the second mode shape is predominantly second bending, the strut will undergo flutter in a predominantly first bending mode shape. This type of flutter is called bending flutter, and the struts are known as bending-type struts. If the second mode shape of the strut is predominantly first torsion, the strut will undergo flutter in a predominantly first torsion mode shape. This type of flutter is called torsional flutter, and the struts are known as torsion-type struts.

Struts with little or no tip weighting are usually bending-type struts, and those with relatively heavy pods are usually torsion-type struts. There is a transition region in which the second vibration mode of a strut has strong components of both second bending and first torsion, with neither predominating. Struts in this region have moderately weighted pods or medium to large foils. It is impossible to deduce which flutter mode will occur in this transition region.

Typical hydroelastic mode characteristics for bending-type and torsion-type struts are shown in Figures 3 and 4, respectively. These drawings were adapted from published calculations and experimental results.[1]

As shown in Figure 3, bending flutter corresponds to an instability in the "new mode," a mode which does not exist at low speed. The new mode first occurs, highly damped, at intermediate speed and decreases rapidly in damping just below the critical flutter speed U_F. The new mode has a first bending mode shape. Its frequency remains very low and close to that of Mode 1. Because of its damping behavior, the new mode cannot be detected in practice until shortly before flutter is encountered.

An entirely different hydroelastic mode is responsible for torsional flutter, as shown in Figure 4. The damping of Mode 2 remains low throughout the subcritical speed range, rising only slightly above its zero speed value before becoming negative. Flutter occurs in a predominantly first torsion mode shape.

---

[1]Besch, P.K. and Y.-N. Liu, "Bending Flutter and Torsional Flutter of Flexible Hydrofoil Struts," Ninth Symposium on Naval Hydrodynamics, Paris, France (Aug 1972); also NSRDC Report 4012 (Feb 1973). A complete listing of references is given on pages 73–76.
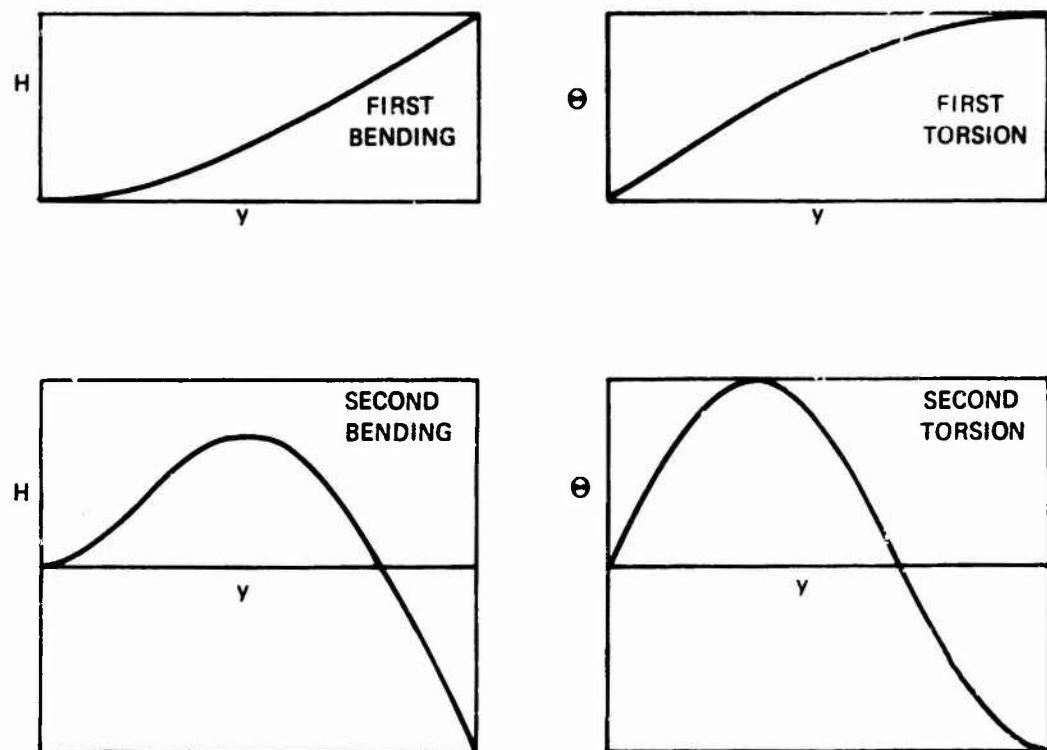
Figure 2 — Uncoupled Mode Shapes of Cantilever Beam

5
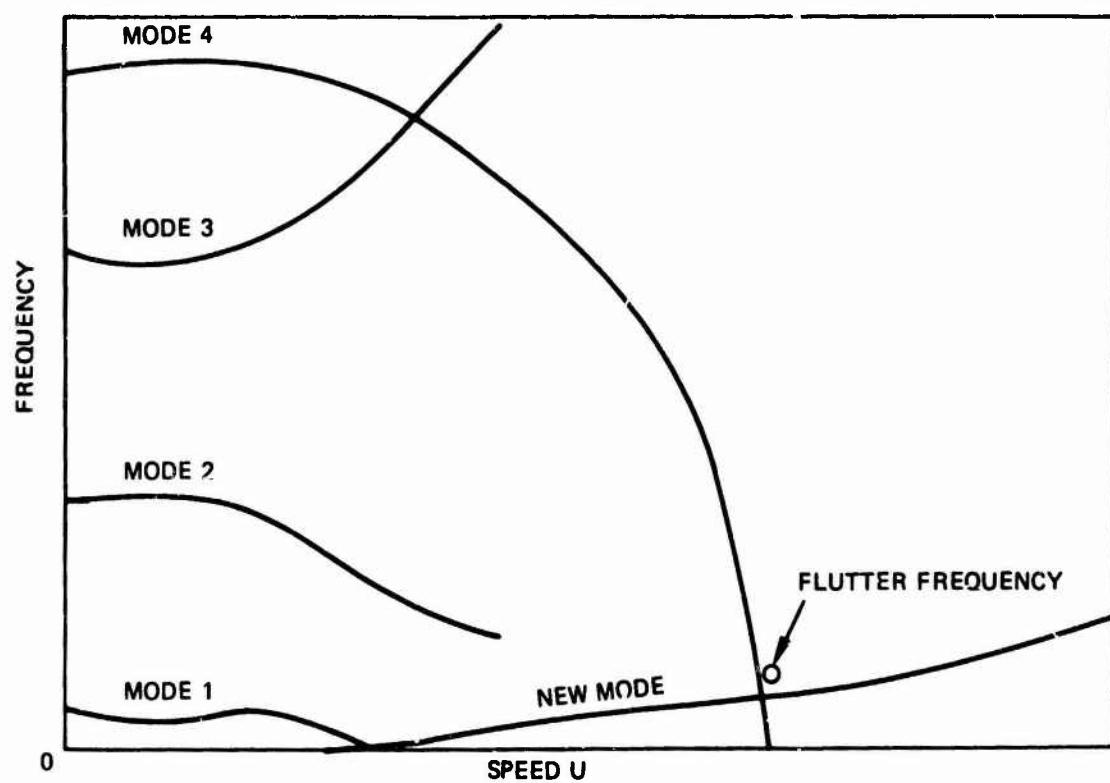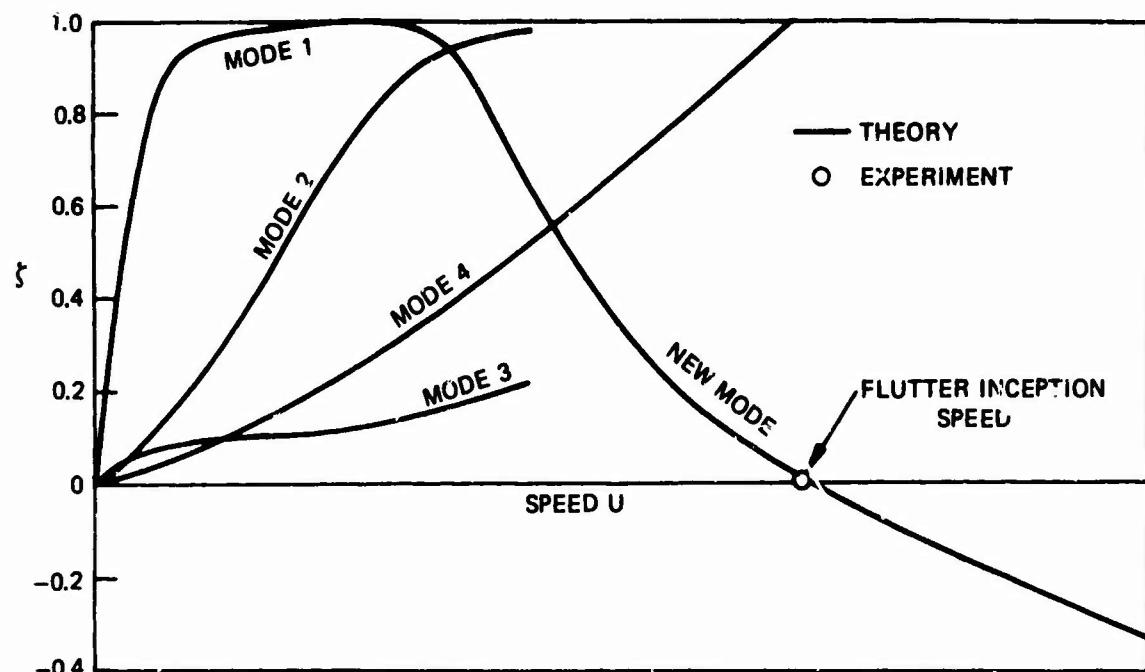
Figure 3 – Typical Hydroelastic Mode Characteristics for Bending-
Type Struts
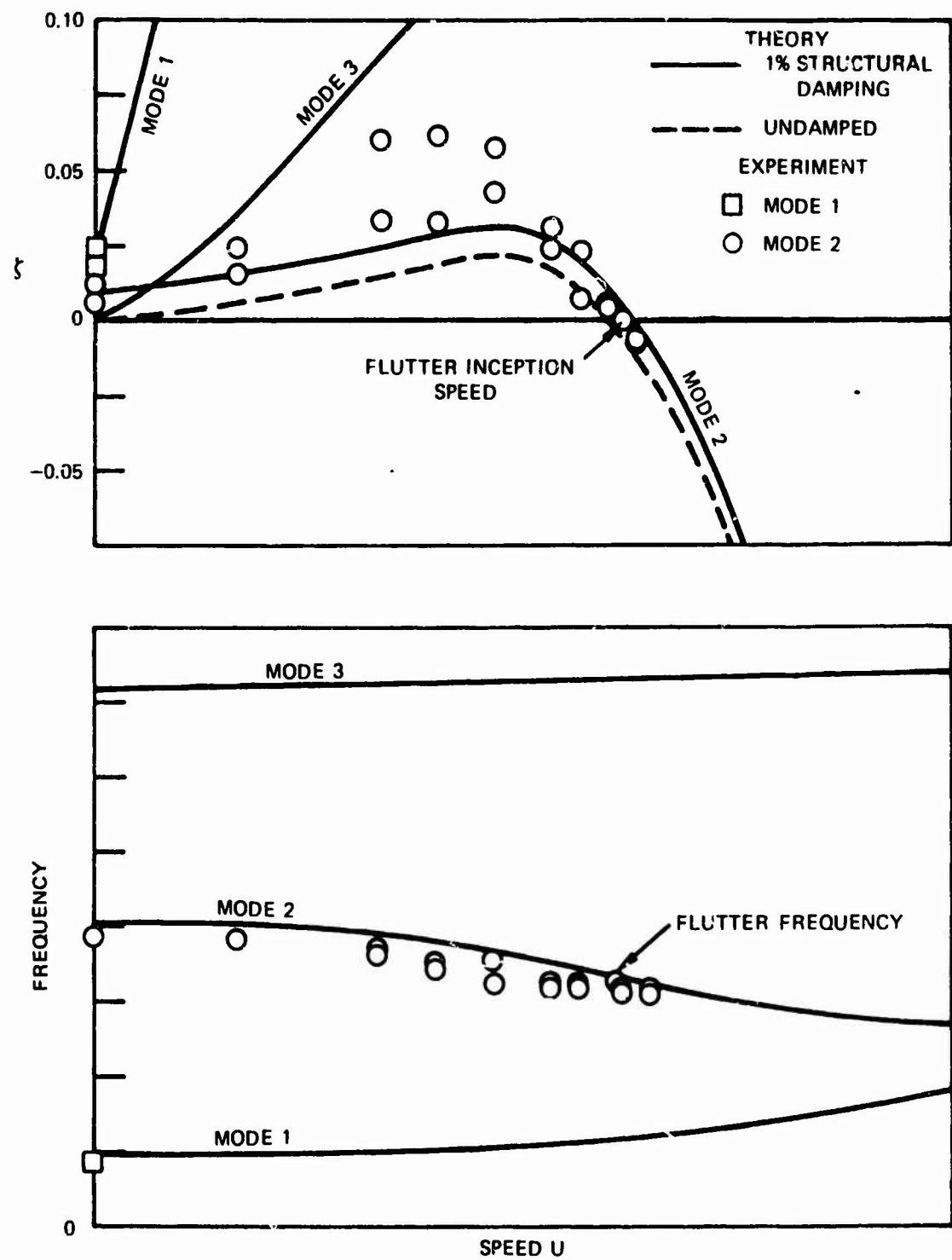
Figure 4 – Typical Hydroelastic Mode Characteristics for Torsion-
Type Struts

7

Calculations imply that at very high speeds a "new mode" appears in the torsional flutter region. As strut characteristics vary toward the bending region, the stability of Mode 2 increases and that of the new mode decreases. The transition from torsional flutter to bending flutter appears to involve a crossover of the critical flutter boundaries of these two modes.

Strut system characteristics are composed of inertial, elastic, and damping characteristics. The change from bending flutter to torsional flutter occurs as a result of inertial and elastic changes in the strut system. Damping is not usually considered to be variable. Inertial changes have a complicated effect on flutter speed; these are qualitatively well understood for strut-pod systems and less so for T-foils. Effects of elastic changes are only approximately known.

Effect of Changing System Inertia

To some extent, important system inertial properties can be summarized in the parameter generalized mass ratio μ. This parameter is the ratio of structural and fluid inertia for a given motion of the strut-fluid system. Generalized mass ratios have been calculated for first bending modes of a T-foil by Mitchell and Rauch.[2] To permit a simple calculation, approximations have been derived by assuming pure bending motion and pure torsional motion to simulate bending flutter and torsional flutter, respectively.[1] For bending motion of strut-pod systems,

$$\mu_{bending} = \frac{M_{strut} + M_{pod}}{M^*_{strut} + M^*_{pod}}$$

where $M^*_{strut} = \pi \rho c^2 \, \ell/4$.

For torsional motion of strut-pod systems,

$$\mu_{torsion} = \frac{I_{y,\,strut} + I_{y,\,pod}}{I^*_{y,\,strut} + I^*_{y,\,pod}}$$

where $I^*_{y,\,strut} = \dfrac{\pi \rho c^4 \ell}{16} \left(\dfrac{1}{8} + \left(\dfrac{2x_{ea}}{c} - 1 \right)^2 \right)$.

---

[2]Mitchell, L. and F.J. Rauch, Jr., "Dynamic Tests of the 1/4-Scale Models of the 80-Knot Transiting Strut-Foil Systems for the FRESH 1 Hydrofoil Test Craft," Grumman Aircraft Engineering Corporation, Contract NObs 86826 (Aug 1964).

The expressions given for strut added mass M^*_{strut} and added moment of inertia $I^*_{y,strut}$ apply to struts of uniform chord c and elastic axis location x_{ea}. Pod added mass M^*_{pod} and added moment of inertia $I^*_{y,pod}$ were approximated in the present work by values given by Kennard[3] for prolate spheroids having lengths and maximum diameters equal to those of the pods.

Model results indicate that bending-type struts with solid cross sections undergo bending flutter for values of $\mu_{bending}$ between 0.1 and 0.66. Flutter speeds for this mode of flutter increase monotonically as $\mu_{bending}$ increases. Flutter frequencies are low; reduced frequencies k_{nf} are near 0.1. Torsion-type struts with solid sections undergo torsional flutter for values of $\mu_{torsion}$ between 0.66 and 6.2. Flutter speeds decrease rapidly as $\mu_{torsion}$ increases above 0.66, and they may reach a minimum at some higher value of $\mu_{torsion}$. Reduced frequencies k_{nf} are near 1.0. Flutter speeds are generally lower and flutter frequencies higher than for bending-type struts. These flutter speed relationships are shown in Figure 5.

By implication from Figure 5, the most stable inertial configuration of a strut system is that which places the strut on the boundary between bending flutter and torsional flutter. This condition occurs when the first torsion and second bending frequencies are equal. Consequently, the flutter speed of a strut with a relatively heavy pod can be raised by lightening the pod or by attaching a high aspect ratio foil.

Effect of Changing System Stiffness

System elastic properties determine the value of mass ratio at which the bending and torsional flutter boundaries intersect as well as the magnitude of flutter speed at a given μ. For thin, solid-section struts with blunt-based profiles, the intersection between bending and torsional flutter occurs at $\mu = 0.66$. Solid struts with airfoil-shaped profiles or struts constructed of spars, ribs, and skin are expected to have approximately the same flutter boundary intersection, but these have not been investigated as thoroughly. This intersection appears to be affected by elastic axis location and the ratio of EI to GJ. For otherwise similar systems, flutter speed magnitudes are related to the magnitudes of EI and GJ.

---

[3]Kennard, E.H., "Irrotational Flow of Frictionless Fluids, Mostly of Invariable Density," David Taylor Model Basin Report 2299, pp. 390–392 (Feb 1967).
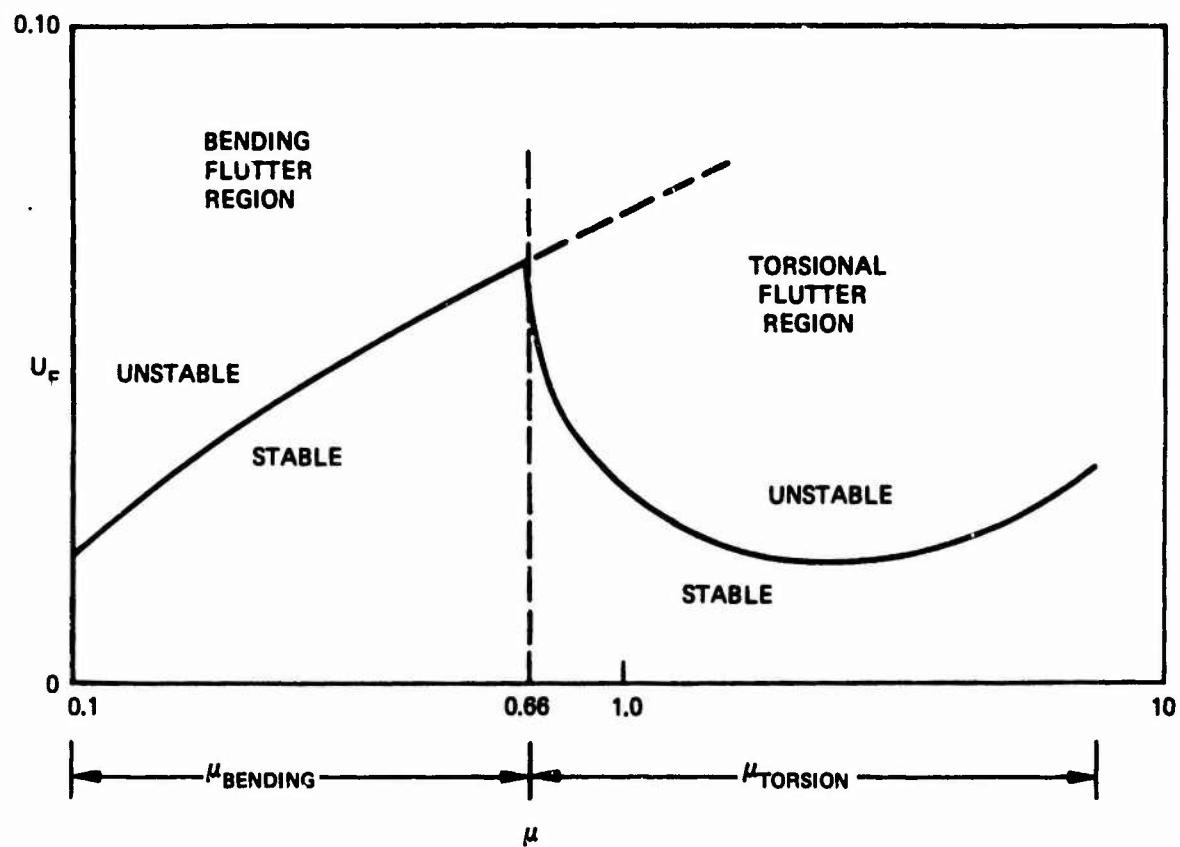
Figure 5 – Variation of Flutter Speed U_f as a Function of Generalized
Mass Ratio μ for Simple Struts and Struts with Pods

(Value of mass ratio at intersection of bending and torsional flutter modes is determined by
elastic and inertial characteristics of structure; 0.66 occurs for solid section struts with thin,
blunt-based profiles.)

Effect of Changing Structural Damping

Structural damping gives a vertical offset to the hydrodynamic damping curve, thereby affecting the resulting flutter inception speed at which total damping becomes zero. The unstable hydroelastic mode in bending flutter has a rapid decrease in damping near flutter and, therefore, is little affected by changes in structural damping. In contrast, torsional flutter speeds are sometimes very sensitive to changes in structural damping because hydrodynamic damping is low at all speeds. The effect of adding a measured value of structural damping to the hydrodynamic damping predicted for the torsional flutter mode is shown in Figure 4.

Flutter has been obtained experimentally for a large number of strut models at speeds ranging from 5.9 to 116 knots. Most of the data are for struts with blunt-based profiles. These struts appear to undergo flutter in the same mode as struts with subcavitating airfoil-shaped profiles but at different speeds.

DIVERGENCE

Divergence is static instability of a lifting-surface structure traveling through a fluid. It occurs when steady elastic deformations of a structure lead to increases in hydrodynamic loading. The divergence speed corresponds to the condition in which the increase in hydrodynamic loading is exactly balanced by the increase in elastic force. Theoretically, infinite deflections occur at higher speeds. In practice, structures yield well before the divergence speed is reached.

There are four common misconceptions about divergence. First, divergence is not simply a "strength problem." Any failure due to approaching divergence can be avoided by sufficiently increasing the stiffness of the structure, but the failure is a result of elastic deflections which change the loading on the structure. Any design procedure must include the elastic response of the structure to the applied loading. This can be done either iteratively or, more efficiently, by making a stability calculation similar to a buckling analysis. The stability boundary is independent of initial angle of attack although angle of attack will affect the speed at which yield occurs.

Second, structures cannot be operated at speeds "up to" the divergence speed. When a divergence instability is present, deflections increase extremely rapidly over the last one-third of the speed range below the divergence speed. The large deflections will hamper operational characteristics of hydrofoil struts, will decrease fatigue lifetime when oscillatory loading is involved, and will cause yielding well below the divergence speed.

11

Third, struts cannot be assumed to have an aerodynamic center location at quarter-chord. This assumption has led designers to conclude that the divergence speed of a strut was infinite when actually it was finite. Divergence analysis requires the use of lifting-surface theory to calculate the aerodynamic center on the strut.

Fourth, structural failure can occur in either bending or torsion, depending on the particular stresses involved. This happens because the flow produces both a lift and a moment, each of which is influenced by variation in angle of attack. Prediction of actual failure conditions requires a detailed stress calculation for the structure as a function of speed.

FLAP REVERSAL

Flap reversal, a form of control surface reversal,[4] is the reversal in direction of the increment in lift induced by a flap deflection. The reversal occurs when the effect on lift of foil elastic deflection cancels the effect of a flap deflection. Specifically, when a trailing-edge flap is deflected downward, the resulting hydrodynamic twisting moment tends to reduce the foil angle of attack. Since the torsional rigidity of the foil is independent of speed but the twisting moment increases with the square of the speed, the net lift increment will be zero at some critical speed, namely the flap reversal speed. This condition obviously would limit controllability of the craft. Both the absence of flap reversal on full-scale craft and preliminary design calculations for the PHM craft show that hydrofoils have flap reversal speeds well above the subcavitating speed range. Calculated flap reversal speeds are considered sufficiently accurate for subcavitating hydrofoil design. Flap reversal on cavitating foils involves substantially different loading, different foil structures, and higher speeds and has not been adequately studied.

RECOMMENDED HYDROELASTIC DESIGN PROCEDURE

For design purposes, a T-foil must be shown to be free from both flutter and divergence independently of each other. Both modes of instability must be investigated for all flow conditions because the speeds at which failure occurs in each may change their

---

[4]Scanlan, R.H. and R. Rosenbaum, "Aircraft Vibration and Flutter." Dover Publications, Inc., New York (1968).

12

relative positions at different depths, angles of attack, etc. If a model is used, failure may occur at different fractions of divergence speed on model and prototype because of structural differences.

INITIAL DESIGN

Subcavitating Systems

In view of the large number of stable T-foils in operation, initial subcavitating designs should be based on the characteristics of existing systems. Such systems define "design families" composed of geometrically similar parts and similar materials which will also be stable. Only the size must be specified, according to the loading expected from craft displacement, maneuvering requirements, and sea conditions. Existing subcavitating T-foils are listed in order of increasing chord length in Table 1.

If existing designs are not suitable, it is recommended that existing configurations be modified in the light of known parameter trends.

Cavitating Systems

All hydrofoil structures will cavitate at speeds above 50 knots. No design information is available for ensuring stability of full-sized T-foils above 62 knots, the maximum speed attained by the DENISON.[5] The FRESH-1 demonstration T-foils are not considered relevant because of their relatively small size, as indicated in Table 2. The design of cavitating systems requires producing a structure of maximum stability under subcavitating conditions and carefully avoiding the cavitation patterns which are known to be destabilizing for some systems. Initial designs for operation above 62 knots must be regarded as highly tentative until their stability has been confirmed by model experiments or operational experience.

---

[5]Schaffer, A.P., "Flutter Flight Testing of a High Speed Hydrofoil Craft—The H . DENISON," Grumman Aircraft Engineering Corporation Report FT-HYD-la.1 (Apr 1963).

TABLE 1 – EXISTING SUBCAVITATING T-FOILS

Craft	Strut-Foil System	Strut Chord in.
PGH-2 (TUCUMCARI)	Forward	36
PGH-1 (FLAGSTAFF)	Main	40
PGH-2 (TUCUMCARI)	Aft	45–55.6
PCH (HIGH POINT)	Forward	51
PGH-1 (FLAGSTAFF)	Tail	60
AGEH (PLAINVIEW)	Tail	72
AGEH (PLAINVIEW)	Main	141

TABLE 2 – EXISTING CAVITATING T-FOILS

Craft	Strut-Foil System	Strut Chord in.
FRESH-1	Demonstration Centerline	25.7
FRESH-1	Demonstration Outboard	25.7
DENISON	Tail	58.4–145

14

EVALUATION OF FIXED DESIGN

Three techniques can be used to estimate the flutter and divergence stability of a proposed T-foil design. It is helpful to an analyst to use as many of the techniques as possible in studying a configuration.

Model Experiments

Accurate flutter speed estimates can be obtained from experiments with a flutter model of a prototype. Typical subcavitating prototype structures can be simulated by a simplified, solid-section model that permits useful flutter speed estimates to be obtained at moderate cost. Ventilated systems may require a model which is slightly more complex. Models can be built at considerably greater cost for studying prototype structures in detail or for studying unusual structures.

The use of models for determining divergence characteristics would not be productive unless analytical methods are invalidated by an unusual design or by the presence of significant amounts of cavitation or ventilation.

Operational experience of the stability of one T-foil in a design family may be regarded as a model test for other size systems.

Theoretical Analysis

Theoretical predictions of flutter speeds of T-foils cannot be relied on since adequate data are not available for evaluation. However, theoretical analysis can provide valuable information about the probable flutter mode and can give qualitatively useful guidance on system stability.

Theoretical divergence predictions for subcavitating flow are quite accurate and suitable for full evaluation of system stability. Divergence predictions for cavitating flow have not been evaluated.

Full-Scale Experiments

Full-scale flutter experiments provide full assurance of system stability. The intent is to avoid structural failure by detecting decreasing damping before instability occurs. This may be feasible for torsional flutter but may not be for bending flutter.

15

Full-scale flutter testing techniques are not adequately developed at the present time. Stability measurements require a method of structural excitation in order to measure damping. None of three demonstrated methods appears completely satisfactory. Impulsive excitation by log impact, achieved randomly and unintentionally on the AGEH main T-foil, produced excellent torsional decay signals but in an uncontrolled manner. The DENISON was reported to have achieved sufficient excitation by maneuvering and by crossing a wake.[5] These techniques may be inaccurate because the forms of the excitation are needed for proper analysis and these are not known. For maximum accuracy, an excitation system should be attached to the strut, pod, or foil or else a known impulsive load should be applied externally. Evaluation of flutter stability by full-scale testing would therefore entail development of an excitation technique.

SCALING LAWS

Scaling laws or laws of similarity must be applied to extrapolate information from existing designs or model studies to a new design. It is possible to formulate similarity conditions for two systems that are expected to be kinematically similar. However, it is not now possible to state any general stability boundaries in quantitative form without a great deal more experimentation. For this reason, it is hoped that the following relationships will be useful in the interim.

SYSTEM PARAMETERS

System parameters are required both to describe a given T-foil system and to provide a basis for deriving scaling laws. The hydroelastic analysis of T-foils is carried out by using virtually the same parameters as for aeroelastic analysis of airplane wings[6] but with additional parameters for free-surface effects and cavitation. Specifically, hydrofoil struts and foils can be represented as beams by using straight elastic axes determined by local shear center locations. Structural and hydrodynamic properties can be given as spanwise distributions of chordwise sectional properties. Chordwise sections of swept structures can be taken either streamwise or in a direction normal to the elastic axis; axis-normal sections are used in this report.

---

[6]Bisplinghoff, R.T. et al., "Aeroelasticity," Addison-Wesley Publishing Company, Inc., Cambridge, Massachusetts (1955).

16

The parameters used to describe a T-foil are listed in the appendix.

NONDIMENSIONAL SCALING RATIOS

T-foils which are different in size, material, or other characteristics will have equal nondimensional flutter and divergence boundaries when all nondimensional parameter ratios are the same. Under these conditions, the flutter speeds and frequencies obtained for one of the systems can be used to determine flutter speeds and frequencies for the other systems. Divergence speeds can be similarly scaled, but the scaling calculation does not generally indicate the speed of structural failure. Nondimensional flutter and divergence parameter ratios for subcavitating and cavitating T-foils are given in the appendix. The scaling relationships involving system size and stiffness are included in the discussions of parameter trends.

FLUTTER OF SUBCAVITATING STRUT SYSTEMS

KNOWN PARAMETER TRENDS

The following discussion applies primarily to subcavitating systems with streamlined, airfoil-like profiles. The parameters of some cavitating systems, notably those with blunt-based profiles which are naturally ventilated aft of the section, have similar trends. Differences in flutter characteristics of subcavitating and cavitating systems are discussed in another section of this report.

Flutter Mode

Strut systems undergo both bending flutter and torsional flutter. Bending flutter occurs when the second bending frequency is lower than the first torsion frequency in water. Torsional flutter occurs when the reverse is true.

17

Inertial Parameters

The inertia characteristics of a T-foil can be expressed in terms of generalized mass ratio μ. The dependence of flutter speed on μ is shown in Figure 5. The most stable inertial configuration for a strut system occurs on the boundary between bending flutter and torsional flutter.

Bending Flutter Region. As shown by the data in Figure 6, flutter speed in the bending flutter region increases monotonically as $\mu_{bending}$ increases.[1,7-10] Therefore, flutter speed increases as the mass of the strut m increases and as the submergence ℓ decreases. It is further known[1] that flutter speed increases as the sweep parameter κ increases, so that increasing sweep angle Λ or decreasing strut length L will stabilize a strut. However, bending flutter probably does not occur when struts are unswept, implying that the dependence of flutter speed on Λ is reversed at low sweep angles. Experimental evidence for these relationships has been obtained almost entirely from struts with blunt-based profiles.

Torsional Flutter Region. For most practical hydrofoils in the torsional flutter region, flutter speed decreases rapidly as $\mu_{torsion}$ increases.[1] A minimum flutter speed will always occur if submergence is decreased. This relationship is demonstrated in Figure 5 and shown experimentally[1,8,10-12] in Figure 7. Therefore, the effects on flutter speed of moment of inertia, pod size, and other parameters in $\mu_{torsion}$ are opposite on either side of the minimum flutter speed. It is expected, however, that nearly all practical configurations will be to the left of the minimum in the flutter speed curve.

[7]Hilborne, D.V., "The Hydroelastic Stability of Struts," Admiralty Research Laboratory (Great Britain) Report ARL/R1/G/HY/5/3 (1958).

[8]Huang, T.T., "Experimental Study of a Low Modulus Flutter Model for Strut-Foil-Pod Configurations," Hydronautics, Inc. Technical Report 459-2 (Jul 1967).

[9]Squires, C.E., Jr., "Hydrofoil Flutter, Small Sweep Angle Investigation—Final Report," Grumman Aircraft Engineering Corporation Report DA Nonr-3989.3 (Nov 1963).

[10]Baird, E.F. et al., "Investigation of Hydrofoil Flutter—Final Report," Grumman Aircraft Engineering Corporation Report DA 1⌐ 480-3 (Feb 1962).

[11]Abramson, H.N. and G.E. Ransleben, Jr., "An Experimental Investigation of Flutter of a Fully Submerged Subcavitating Hydrofoil," J. Aircraft, Vol. 2, No. 5, pp. 439—442 (Sep—Oct 1965).

[12]Besch, P.K. and Liu, Y.-N., "Flutter and Divergence Characteristics of Four Low Mass Ratio Hydrofoils," NSRDC Report 3410 (Jan 1971).

Figure 6 — Experimental Flutter Speed U_f as a Function of Bending Mass Ratio $\mu_{bending}$ for Solid-Section, Blunt-Based Struts

19
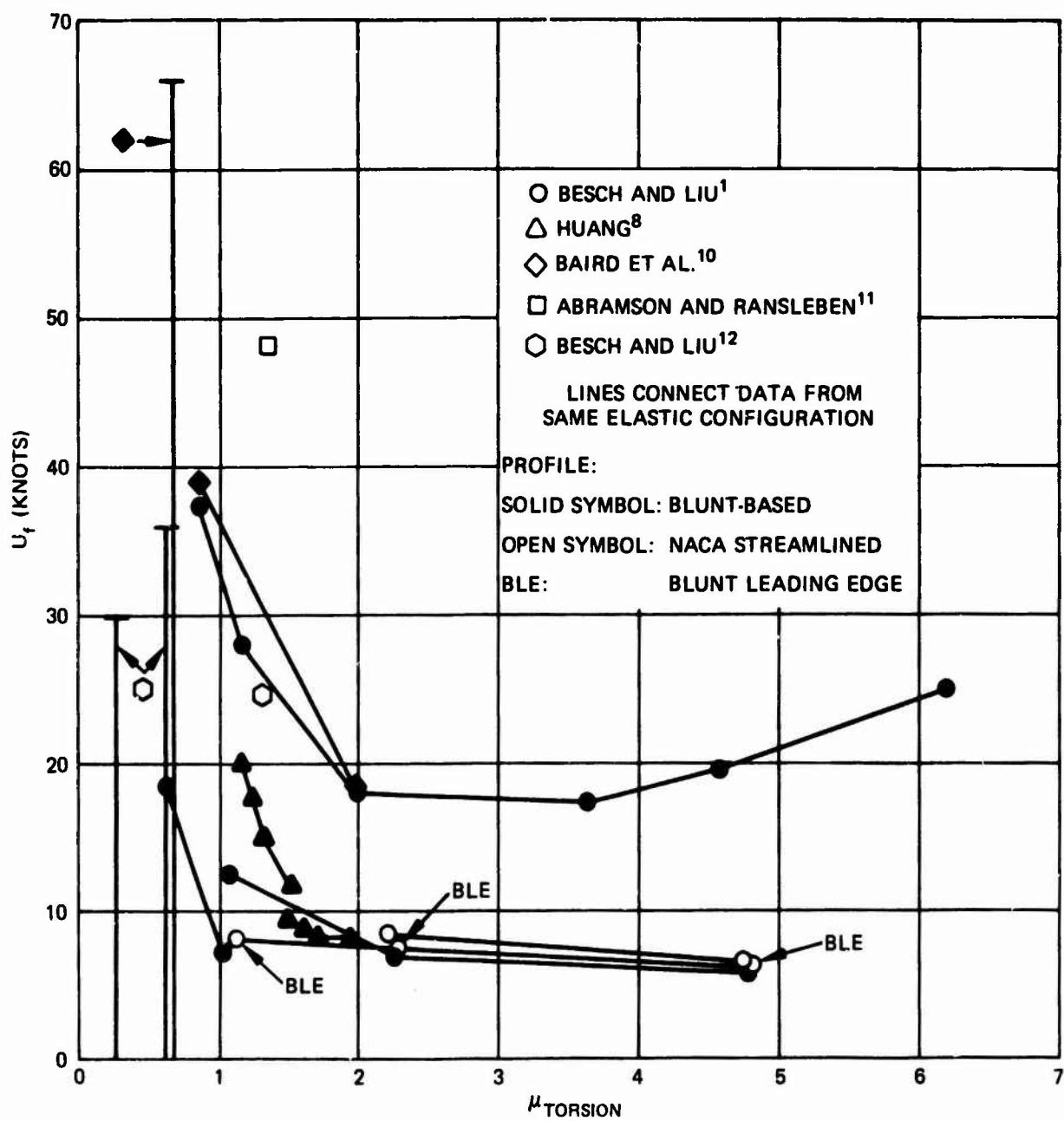
Figure 7 — Experimental Flutter Speed U_f as a Function of Torsional
Mass Ratio $\mu_{torsion}$ for Torsion-Type Struts

Model data[1,11,12] for both simple struts and for a strut with an attached pod exhibited an increase in flutter speed as model inertia was decreased; see Tables 3–6. When the density of the smaller strut family was reduced, the flutter speed increased from 24.7 knots to a value above 36 knots (Tables 3 and 4). These struts remained in the torsional flutter region at low densities because their elastic properties were concentrated in a spar of unusually low torsional flexibility. A strut with a large, heavy pod, described in Tables 5 and 6, exhibited an increase in flutter speed when pod mass was decreased.

It is useful to note that a minimum also occurred in the value of reduced flutter speed $2U_f/c\omega_\alpha$ as a function of $\mu_{torsion}$. The data in Figure 7 have been replotted in Figure 8 to illustrate this dependence. Airfoil data,[13] also plotted in Figure 8, showed similar behavior. The minimum value of reduced flutter speed for hydrofoils occurred between mass ratios of 2.0 and 3.0. The lowest value of reduced flutter speed yet obtained for streamlined or blunt-based struts has been 0.757. A rough estimate of the minimum flutter speed for struts with elastic properties similar to those already tested can be made from the relation $2U_f/c\omega_\alpha > 0.8$ where ω_a is the frequency of the first torsional vibration mode in air. Actual flutter speeds can be many times larger than this minimum.

Elastic Parameters

The elastic characteristics of a T-foil, which include bending stiffness EI, torsional stiffness GJ, and elastic axis location x_{ea}, affect the value of μ at which bending flutter and torsional flutter boundaries intersect as well as the magnitude of flutter speed in each region. Changes which move the second and third vibration mode frequencies closer together shift the system toward the boundary between bending and torsional flutter.

Size and Stiffness

The flutter speed of a given configuration, referred to as the model, can be used to determine the flutter speed of a different configuration, referred to as the prototype, if all dimensionless parameters given in the appendix are equal for the two configurations. Both

---

[13]Woolston, D.S. and G.E. Castile, "Some Effects of Variations in Several Parameters Including Fluid Density on the Flutter Speed of Light Uniform Cantilever Wings," NACA TN 2558 (1951).

TABLE 3 – DIMENSIONED PARAMETERS FOR SUBCAVITATING STRUT FLUTTER MODELS IN FRESH WATER

Strut	Abramson and Ransleben Data[11]	Besch and Liu Data[12]		
		Model 1	Model 2	Model 4
L, in.	30.0	15.0	15.0	15.0
c, in.	12.0	6.0	6.0	6.0
Λ, deg	0.0	0.0	0.0	0.0
x_{ea}, in.	3.0	1.5	1.5	1.5
x_{cg}, in.	6.14	3.07	3.07	3.07
m, lb/in.	4.04	0.983	0.465	0.206
I_{my}, lb-in.	74.5	4.49	2.10	0.938
EI, lb-in.^{2}	3.40×10^6	5.69×10^4	5.53×10^4	5.67×10^4
GJ, lb-in.^{2}	9.73×10^5	1.92×10^4	1.64×10^4	1.56×10^4
Profile:	NACA 16-012	NACA 16-012	NACA 16-012	NACA 16-012
Flutter Condition				
ℓ, in.	30.0*	15.0*	15.0*	15.0*
U_f, knots	48.1	24.7	> 36**	> 30
f_f, Hz	17.5	20.5	--	--
Mode Shape	Torsion	Torsion	--	--

*Reflecting plate at root.

**Structural failure due to approaching divergence occurred at 36 knots.

TABLE 4 – NONDIMENSIONAL PARAMETERS FOR SUBCAVITATING STRUT FLUTTER MODELS

Strut	Abramson and Ransleben Data[11]	Besch and Liu Data[12]		
		Model 1	Model 2	Model 4
L/c	2.5	2.5	2.5	2.5
AR	5.0	5.0	5.0	5.0
κ	0.0	0.0	0.0	0.0
x_{ea}/c	0.25	0.25	0.25	0.25
x_{cg}/c	0.51	0.51	0.51	0.51
$4m/\pi\rho\,c^2$	0.99	0.963	0.455	0.202
$16\,I_{my}/\pi\rho\,c^4$	0.507	0.489	0.229	0.102
Flutter Condition				
AR	5.0	5.0	5.0	5.0
k_{nf}	0.676	0.772	--	--
$4\,EI/\pi\rho\,c^2\,\omega_f^2\,L^4$	3.27×10^{-2}	2.31×10^{-1}	---	--
$16\,GJ/\pi\rho\,L^2\,\omega_f^2\,c^4$	2.34×10^{-1}	2.16×10^{-1}	--	--
R_{nf}	6.7×10^6	1.7×10^6	--	--
F_{nf}	∞	∞	∞	∞
$\mu_{torsion}$	1.35	1.30	0.610	0.272
$\mu_{bending}$	0.99	0.963	0.455	0.202
ζ_s (Mode 2)	0.02	0.02	0.03	0.05

23

TABLE 5 – DIMENSIONED FLUTTER PARAMETERS
FOR SUBCAVITATING STRUT-POD
FLUTTER MODELS

(From Besch and Liu[1])

Strut		
L, in.	58.4	
c, in.	12.0	
Λ, deg	15.0	
x_{ea}, in.	4.5	
x_{cg}, in.	6.2	
m, lb/in.	0.588	
I_{my}, lb-in.	8.21	
EI, lb-in.^{2}	7.58×10^5	
GJ, lb-in.^{2}	10.4×10^5	
Profile	NACA 16-005	
Pod	Config. A.	Config. B
Length, in.	44.0	44.0
Max. Diameter, in.	6.0	6.0
x_{nose}, in.	16.2	16.2
x_{cg}, in.	22.0	22.0
M, lb	140.0	77.3
I_y, lb-in.^{2}	1.57×10^4	7.07×10^3
Flutter Condition		
ℓ, in.	30.4	30.4
U_f, knots	6.6	8.4
f_f, Hz	2.9	3.5
Mode Shape	Torsion	Torsion

TABLE 6 – NONDIMENSIONAL FLUTTER PARAMETERS FOR SUBCAVITATING STRUT-POD FLUTTER MODELS

(From Besch and Liu[1])

Strut		
L/c	4.87	
AR (to root)	4.54	
κ	0.0551	
x_{ea}/c	0.375	
x_{cg}/c	0.52	
$4m/\pi\rho\,c^2$	0.144	
$16\,I_{my}/\pi\rho\,c^4$	0.0559	
Pod	**Config. A**	**Config. B**
Fineness Ratio	7.33:1	7.33:1
Diameter/c	0.50	0.50
x_{nose}/c	1.35	1.35
x_{cg}/c	1.83	1.83
M_{pod}/M_{strut}	4.08	2.25
$I_{y,pod}/I_{y,strut}$	32.7	14.7
Flutter Condition		
AR (strut wetted area)	2.36	2.36
k_{nf}	0.846	0.802
$4\,EI/\pi\rho\,c^2\,\omega_f^2\,L^4$	0.0186	0.0127
$16\,GJ/\pi\rho\,L^2\,\omega_f^2\,c^4$	2.41	1.66
R_{nf}	9.5×10^5	1.2×10^6
F_{nf}	1.9	2.5
ζ_s (Mode 2)	0.02	0.02
$\mu_{torsion}$	4.75	2.21
$\mu_{bending}$	1.16	0.734

25
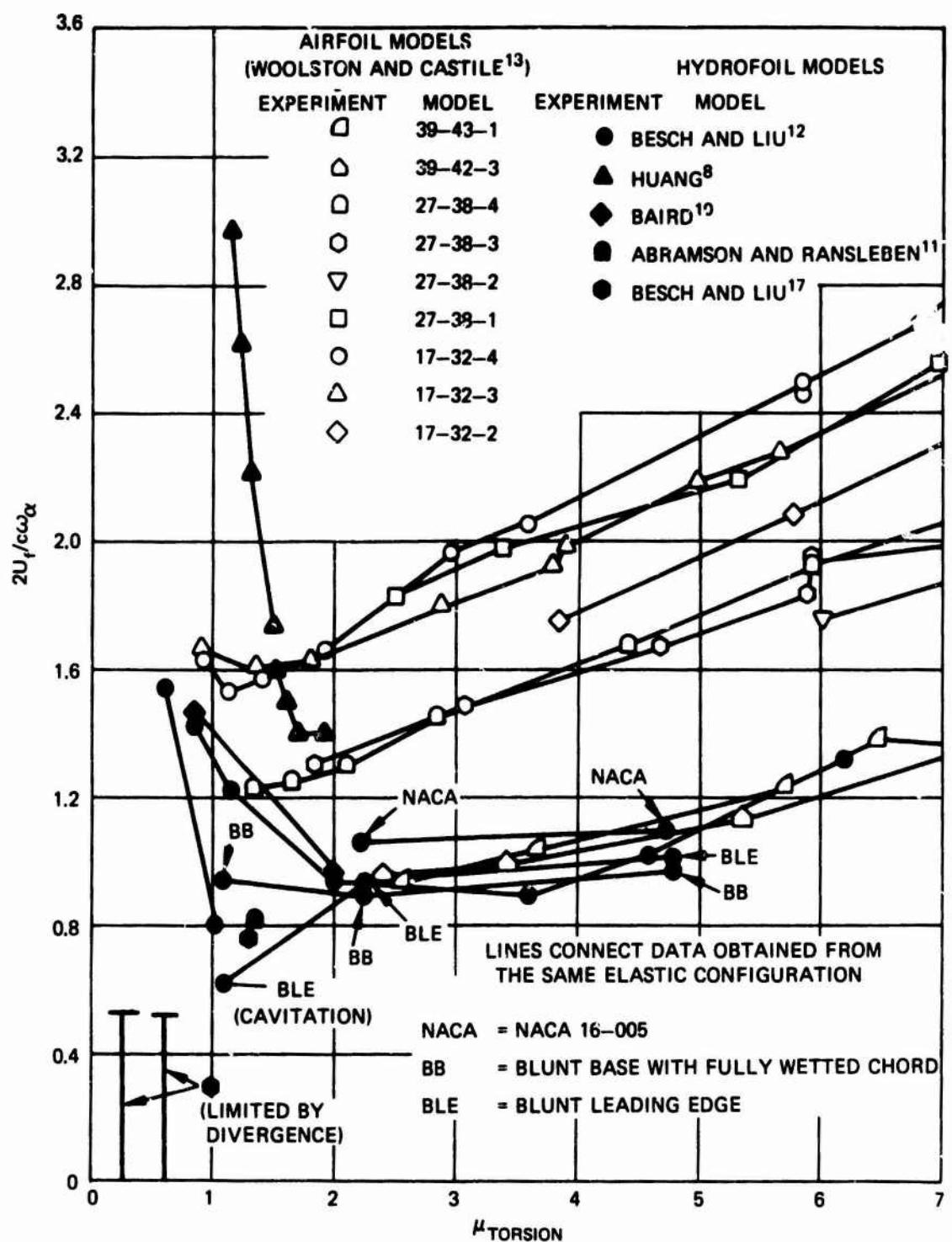
Figure 8 – Reduced Flutter Speed $2U_f/c\omega_\alpha$ as a Function of Torsional Mass Ratio $\mu_{torsion}$ for Torsion-Type Struts

26

size and bending or torsional stiffness can be chosen arbitrarily for a subcavitating prototype. Blunt-based and other ventilated configurations are discussed further in the section on flutter of cavitating strut systems. The flutter speeds of the model and prototype will be related as follows:

$$\frac{U_{f,\,prototype}}{U_{f,\,model}} = \frac{c^2_{model}}{c^2_{prototype}}\sqrt{\frac{EI_{prototype}\,\rho_{model}}{EI_{model}\,\rho_{prototype}}} \quad or \quad \frac{c^2_{model}}{c^2_{prototype}}\sqrt{\frac{GJ_{prototype}\,\rho_{model}}{GJ_{model}\,\rho_{prototype}}}$$

where values of c and EI or GJ are taken from equivalent locations in the two systems.

Effects of Foils

T-foils have been studied much less than struts and strut-pod systems. It is believed that the effect of foils can be explained within the framework of bending and torsional flutter. An attached foil radically changes the inertial characteristics of the strut-fluid system. System elasticity is less strongly affected. Therefore a foil could change the mass ratio of the system and yet have little effect on the flutter boundary (shown in Figure 5) that is characteristic of the strut.

At present, T-foil system characteristics can be estimated only qualitatively from system mode shapes and frequencies. Strong coupling of mode shapes places T-foils generally in a transition region between bending and torsional flutter. Moderate-to-high aspect ratio foils move the second bending frequency of a torsion-type strut close to the first torsion frequency. This result suggests that the foil will raise the flutter speed of a torsion-type strut. The flutter speed of a bending-type strut might be lowered by a foil. Both increases and decreases in flutter speed were observed by Huang[8] when a large foil was attached to a strut with a blunt-based profile. These results are discussed further in the section dealing with cavitating systems.

IMPLICATIONS FOR PROTOTYPE SYSTEMS

The principal implication of available results is that within the size range of existing craft, several T-foils define structural design families which are flutter free throughout the subcavitating speed range or up to 50 knots at small angles of attack. This conclusion is

27

based on observed stability characteristics of both model and full-scale T-foils. Scaling laws required for extending the observed characteristics are supported by a model experiment which successfully reproduced scaling predictions for a system of different size. These results are discussed below.

Validity of Kinematic Scaling

The flutter testing of two nondimensionally similar simple strut models has provided evidence for the validity of kinematic scaling procedures for determining flutter boundaries. The two models[11,12,14] were rectangular, torsion-type struts of aspect ratio 5.0. Model parameters were those for the 30-inch model and Model 1 given in Tables 3 and 4. The scaled flutter speed of the larger strut agrees with its experimental flutter speed within 1 percent when EI is used for scaling, and within 9 percent when GJ is used. Exact agreement is not expected because GJ/EI and $4m/\pi\rho\ c^2$ were not exactly equal for the two struts.

AGEH Main Design Family

The AGEH main T-foil, described in Tables 7 and 8, is now established to be free from flutter throughout the subcavitating speed range. It therefore serves as a parent for a family of T-foils of different size which are also flutter free. The characteristics of this design family will be described following the discussion of experimental results.

Flutter stability of the AGEH main T-foil has been established by both full-scale data and 1/8-scale model data. The full-scale data consisted of stable craft operation through 47 knots plus damping values at two intermediate speeds measured from oscillations excited by impacts with logs.[*] The measured damping values, shown in Figure 9 at 35 and 45.5 knots, were sufficiently high that flutter should not occur in the torsional (second) mode until above 50 knots. Torsional flutter is expected to precede bending flutter in this torsion-type strut system.

A 1/8-scale flutter model[15] of the main foil system, constructed as part of the contract requirements, also provided evidence of flutter stability. Parameters of the model are

---

[14] Ransleben, G.E., Jr., "Experimental Determination of Variation of Hydrofoil Flutter Speed with Mass Ratio," Southwest Research Institute, Contract N00014-69-C-0219 (Apr 1970).

[15] Ransleben, G.E., Jr., "Description of a One-Eighth Scale Flutter Model of the Main Hydrofoil Assembly of the AG(EH) 800 Hydrofoil Research Ship," Southwest Research Institute Project 02-1960 (Dec 1966).

[*] AGEH Full-Scale Trial 71HA211-22 (24 Aug 1971, Voyage 66, Tape AT66B, Time 16:22:27) and Trial 72HA-A241G-31 (31 May 1972, Tape 180B, Voyage 117, Time 10:39:30).

TABLE 7 – DIMENSIONED FLUTTER PARAMETERS FOR FULL-SCALE SUBCAVITATING T-FOILS

Strut	PCH Mod 1	PHM	AGEH Tail	AGEH Main
L, in.	129.6	220.2	278.1	328.6
c, in.	51.0	66.5	72.0	141
Λ, deg	0.0	6.3	0.0	0.0
x_{ea} (3/4 span), in.	14.8	27–33	43.2	45
x_{cg} (3/4 span), in.	23.9	28.3	36	66
m (3/4 span), lb/in.	25	24	19	60
I_{my} (3/4 span), lb-in.	5.2×10^3	1.3×10^4	9.7×10^3	1.0×10^5
EI (3/4 span), lb-in.^{2}	7×10^9	2.0×10^{10}	1.5×10^{10}	1.1×10^{11}
GJ (3/4 span), lb-in.^{2}	9.5×10^9	2.9×10^{10}	1.5×10^{10}	1.1×10^{11}
Profile (3/4 span)	NACA 16-012	NACA 16-012	NACA 16-011	NACA 16-012
Pod				
Length, in.	90	157.5	156	321.7
Max. Diameter, in.	13.5	25	30	49
x_{nose}, in.	24.0	40	41.2	107.1
x_{cg}, in.	18.6	35.4	40	97
M, lb	226	2,351*	875	13,705
I_y, lb-in.^{2}	4.6×10^4	$7.4 \times 10^{5*}$	1.98×10^6	1.25×10^8
Foil				
Area, ft^2	65.6	140.9	60.0	225.0
c_{root}, in.	63.0	93.3	82.4	159.8
Tip Chord, in.	15.7	28.0	24.7	47.9
Full Span, in.	240	335	161	312
Λ, deg	15.0	11.04	35.2	35.2
x_{foil}, in.	12.0	13.2	6.79	51.7
M, lb	4200	7201	2182	8884
x_{cg}, in.	25.3	37.8	48	58
I_y, lb-in.^{2}	1.16×10^7		2.62×10^6	$4.94 \times 10^{7**}$
Profile	NACA 16-309 a = 1.0	NACA 16-206.5 a = 1.0	NACA 16-X08 x = 0.425 a = 1.0	NACA 16-X08 x = 0.39 a = 1.0
Flutter Condition				
ℓ, in.	Not available	Not available	--	96
U_f, knots			Above 50	Above 50
f_f, Hz			--	--
Mode Shape	Not available	Not available	--	--

* Pod inertia includes section of strut enclosed within pod and an estimated 558 lb of enclosed water (pod is flooded).

** About vertical axis; strut elastic axis has 10-deg dihedral.

29

TABLE 8 – NONDIMENSIONAL FLUTTER PARAMETERS FOR FULL-SCALE SUBCAVITATING T-FOILS

| Strut	PCH Mod 1	PHM	AGEH Tail	AGEH Main
L/c	2.54	3.31	3.86	2.33
AR (to root)	2.5	3.3	3.0	2.3
K	0.0	0.033	0.0	0.0
x_{ea} (3/4 span)/c	0.29	0.40–0.50	0.60	0.32
x_{cg} (3/4 span)/c	0.47	0.43	0.50	0.47
$4m$ (3/4 span)/$\pi\rho\,c^2$	0.336	0.189	0.126	0.104
$16\,I_{my}$ (3/4 span)/$\pi\rho\,c^4$	0.105	0.0941	0.0497	0.0348
Pod				
Fineness Ratio	7.1:1	6.3:1	5.2:1	6.6:1
Diameter/c	0.265	0.376	0.417	0.348
x_{nose}/c	0.471	0.602	0.572	0.760
$x_{cg,pod}/c$	0.365	0.532	0.555	0.688
M_{pod}/M_{strut}	0.063	0.30	0.081	0.65
$I_{y,pod}/I_{y,strut}$	0.044	0.42	0.40	1.48
Foil				
c_{root}/c	1.24	1.40	1.14	1.13
AR	6.1	5.5	3.0	3.0
Λ, deg	15.0	11.04	35.2	35.2
τ	0.25	0.30	0.30	0.30
x_{foil}/c	0.24	0.20	0.094	0.37
x_{cg}/c	0.50	0.57	0.67	0.41
M_{foil}/M_{strut}	0.92	1.01	0.20	0.42
$I_{y,foil}/I_{y,strut}$	11.3	39.9	0.52	0.59
Flutter Condition				
AR (strut wetted area)	Not available	Not available	Not available	Not available
k_{nf}				
$4\,EI$ (3/4 span)/$\pi\rho\,c^2\,\omega_f^2\,L^4$	↓	↓	↓	↓
$16\,GJ$ (3/4 span)/$\pi\rho\,L^2\,\omega_f^2\,c^4$				Not available
R_{nf}				above 8.1×10^7
F_{nf}				above 4.3
ζ_s	Not available	Not available	Not available	0.09 (Mode 2)

Figure 9 – Hydroelastic Mode Characteristics for AGEH Main T-Foil

31

given in Tables 9 and 10. This model (shown in Figure 1) was constructed of single spars with independent skin sections and involved considerable expense. The scale model was designed by selecting the desired length and velocity ratios between prototype and model, thus determining model stiffnesses. In this case, the velocity ratio was chosen to produce the same value of Froude number F_n for both systems. This condition was not required, however, at the relatively high values of F_n associated with the system.

Model vibration characteristics were in fairly good agreement with full-scale characteristics but did exhibit some discrepancies.[16] The model was relatively more flexible in torsion than the prototype and had 2 percent less structural damping in the second, or unstable mode. When the model frequency was appropriately scaled, the greater flexib' ty of the model was revealed by the fact that its torsional frequency (at 29-percent submergence) was lower than that of the prototype (at 80-percent submergence).

The structural damping in the second mode of both model and prototype, 7 and 9 percent, respectively, was unusually high for winglike structures. Such high damping raises the flutter speed of the second mode substantially. It is encouraging that both model and prototype developed high Mode 2 damping despite differences in construction because it suggests that structural damping is to some extent simulated even though it is usually not a design parameter.

Figure 9 shows model frequency data obtained from mechanical impedance measurements made at NSRDC during flutter testing (unpublished data from D.S. Cieslowski). Frequencies have been converted to full-scale values. Damping values obtained from impedance measurements showed excessive scatter and are not given. The damping ratio at zero speed was obtained by line cut excitation.

At 33 knots, the model encountered a flutter instability at a frequency equal to that of the second mode at zero speed. The strut was 29-percent submerged, corresponding to design flying height. The instability damaged the model and precluded testing at other submergence depths. Previous results[1] indicate that minimum torsional flutter speeds of strut-pod models occurred at 50-percent submergence but that one T-foil model had a minimum flutter speed at 100-percent submergence. It is concluded that the minimum flutter speed of the AGEH model is probably lower than 33 knots and that it would occur at a deeper submergence.

This model result correpsonds to a scaled flutter speed of 93 knots for the full-scale AGEH main T-foil system. This prediction is valid only for subcavitating flow conditions

---

[16]Peoples, J.R., "Frequencies and Damping of Full Scale Hydrofoils by "Pluck Test" Methods," 43rd Shock and Vibration Bulletin, Shock and Vibration Information Center, Naval Research Laboratory, Washington, D.C. (Jun 1973); also indicated by D.S. Cieslowski of NSRDC in a private communication.

TABLE 9 – DIMENSIONED FLUTTER PARAMETERS FOR 1/8-SCALE AGEH MAIN T-FOIL FLUTTER MODEL

Strut		Foil	
L, in.	41.1	Area, in.^{2}	506
c, in.	17.6	c_{root}, in.	20.0
Λ, deg	0.0	Tip Chord, in.	6.0
x_{ea} (3/4 span), in.	5.6	Foil Span, in.	39.0
x_{cg} (3/4 span), in.	8.3	Λ, deg	35.2
m (3/4 span), in.	0.916	x_{foil}, in.	6.43
I_{my} (3/4 span), lb-in.	2.98	M, lb	16.9
EI (3/4 span), lb-in.^{2}	3.28×10^6	x_{cg}, in.	7.3
GJ (3/4 span), lb-in.^{2}	3.28×10^6	I_y, lb-in.^{2}	$1.47 \times 10^{3}*$
Profile (3/4 span)	NACA 16-012	I_ϕ, lb-in.^{2}	
		Profile	NACA 16-X08 x = 0.390 a = 1.0
Pod			
Length, in.	40.2	**Flutter Condition**	
Max. Diameter, in.	6.1	ℓ, in.	12.0
x_{nose}, in.	13.4	U_f, knots	33
x_{cg}, in.	12.1	f_f, Hz	10.6
M, lb	26.1	Mode Shape	Torsion
I_y, lb-in.^{2}	$3.73 \times 10^{3}*$		
I_ϕ, lb-in.^{2}			

*About vertical axis; strut elastic axis has 10-deg dihedral.

33

TABLE 10 – NONDIMENSIONAL FLUTTER PARAMETERS FOR
1/8-SCALE AGEH MAIN T-FOIL FLUTTER MODEL

Strut		Foil	
L/c	2.34	c_{root}/c	1.16
AR (to root)	2.3	AR	30
κ	0.0	Λ	35.2
x_{ea} (3/4 span)/c	0.32	τ	0.30
x_{cg} (3/4 span)/c	0.47	x_{foil}/c	0.3S7
$4m$ (3/4 span)/$\pi \rho \, c^2$	0.104	x_{cg}/c	0.41
$16 \, I_{my}$ (3/4 span)/$\pi \rho \, c^4$	0.0348	M_{foil}/M_{strut}	0.42
		$I_{y,foil}/I_{y,strut}$	0.59
Pod		$I_{\phi,foil}/I_{\phi,pod}$	
Fineness Ratio	6.6:1		
Diameter/c	0.347	**Flutter Condition**	
x_{nose}/c	0.761	AR (strut wetted area)	0.68
x_{cg}/c	0.688	k_{nf}	0.88
M_{pod}/M_{strut}	0.65	$4 \, EI$ (3/4 span)/$\pi \rho \, c^2 \, \omega_f^2 \, L^4$	0.0114
$I_{y,pod}/I_{y,strut}$	1.48	$16 \, GJ$ (3/4 span)/$\pi \rho \, L^2 \, \omega_f^2 \, c^4$	0.247
$I_{\phi,pod}/I_{y,strut}$		R_{nf}	6.7×10^6
		F_{nf}	8.1
		ζ_s	0.07

34

and a strut submergence of 29 percent. Subcavitating flow can be maintained only up to approximately 50 knots at small angles of attack; the effect of cavitation on flutter of stream-lined profiles has not been studied. On the basis of previous results,[1] it appears unlikely that flutter speed would decrease as much as 46 percent as submergence increased. Furthermore, the small discrepancies in damping and torsional stiffness between model and prototype would raise the scaled flutter speed. Therefore the AGEH main T-foil is considered flutter free for all subcavitating flow conditions.

A family of similarly flutter-free T-foil designs are obtainable from this result. The family consists of all T-foils constructed of components geometrically scaled from the AGEH system and composed of the same (or equal density and moduli) materials. The section moduli of such T-foils vary as the fourth power of any linear dimension. Therefore, if the structural damping ratios of the second modes are equal, the scaled systems will flutter at the same speed as the AGEH system, according to the scaling relationship presented earlier. This should be confirmed by full-scale vibration tests of future systems. Froude number is not preserved under these conditions, however, and it is expected that scaling would become inaccurate for extremely large systems which correspond to low values of Froude number. Torsional stiffnesses GJ for geometrically scaled systems correspond to the AGEH main design family shown in Figure 10. A more efficient structural design would give greater rigidity for the same weight of material and thus be more stable.

Other Stable Design Families

The AGEH main T-foil serves as a parent for a design family of stable T-foils with relatively heavy pods and moderate aspect ratio foils. All other existing T-foils similarly define different stable families of subcavitating T-foils by virtue of having successfully operated at high subcavitating speeds. Parameters for three such T-foils are given in Tables 7 and 8. The rule of geometric and material similarity can be used to produce equally stable T-foils up to a size at which Froude number is considered too low to be disregarded. The design family for the PCH and PHM struts, shown in Figure 10, gives further indication that maximum stiffness for operational T-foils has probably been reached. Intermediate stiffness families, corresponding, e.g., to the AGEH tail T-foil, can be established by drawing lines parallel to the lines given in Figure 10.

The stability of all operational systems suggests that present design criteria that are not based on hydroelastic considerations do yield T-foils which are sufficiently rigid to preclude flutter and divergence. The design criterion for the PCH Mod-1 forward strut was the ability to withstand full loading on one side of a half-broached foil or, alternatively, a 0.2-g
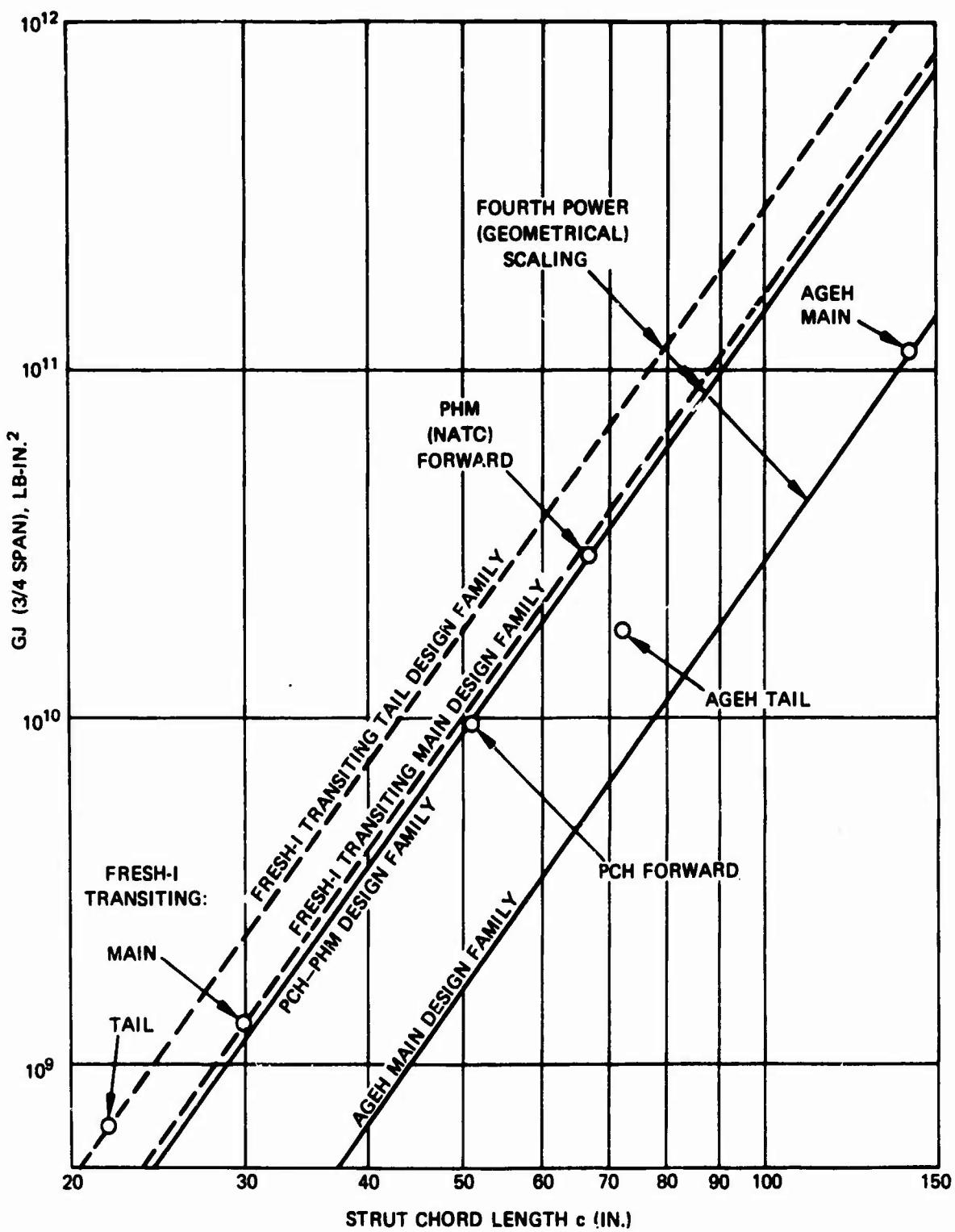
Figure 10 – Torsional Stiffness GJ as a Function of Strut Chord
Length for Geometrically Similar T-Foil Designs

36

strut side load.[17] Thus although present designs, particularly those for the smaller chord PCH and PHM, might be overdesigned for hydroelastic stability, other considerations would prevent weight-saving optimization.

It should be observed that as size increases, the prototype stiffnesses, shown in Figure 10, increase more slowly than geometrically scaled stiffnesses. This trend is due to structural differences in the systems represented. These systems do not necessarily represent the only design alternatives as a function of size. However, if large size struts are constrained by fabrication requirements or other considerations to continue this trend, then the flutter speeds of large members of a design family will decrease as size increases. Therefore, existing design families cannot be assumed to be hydroelastically stable and suitable for use on craft larger than the AGEH until a study is made of the engineering aspects of large-scale strut-foil structures, including the effects of size on other design criteria.

EXPERIMENTAL MODELING TECHNIQUES

Flutter models are extremely valuable for confirming the stability of hydrofoil structures. Because of the present inadequacy of flutter theory, for example, quantitative bending flutter boundaries can be obtained only from model results. If there is any question of flutter instability after a comparison with existing designs and the performance of a modified strip analysis, a model experiment should be conducted before construction is started.

Difficulties in designing successful strut models have been experienced in the past, but these difficulties can now be avoided. It is proposed to use a solid cross section model which is a close but not exact simulation of a prototype configuration. Model requirements are discussed below.

Model Cost

Model cost depends on the complexity of construction. Semimonocoque models can simulate all prototype elastic and inertia characteristics exactly, but at considerable expense. It is therefore proposed to use solid cross section models, which are relatively inexpensive to build.

---

[17]"PCH-1 Mod 1 Detail Design--Structural Summary," The Boeing Company (1969).

Solid Cross Section Parameters

Solid cross sections of streamlined profile can be used to adequately simulate the elastic and inertial properties of most prototype struts and foils under subcavitating flow conditions. The simulation is based on choosing the thickness-to-chord ratio of the model so that the required mass and moment of inertia are produced. The prototype thickness does not have to be simulated exactly so long as cavitation does not occur.

The remaining parameters that must be simulated are inherently well modeled by a solid cross section, namely, center of gravity location x_{cg}/c, elastic axis location x_{ea}/c. and GJ/EI. Characteristic values of these parameters for existing prototype craft and for a solid cross section are given in Table 11. Although prototype values of x_{ea}/c vary widely on either side of the solid section value, the extreme values shown are misleading. The farthest aft location of 60-percent chord, found on the AGEH tail strut, is expected to be avoided in future designs because it leads to unfavorable divergence characteristics. The farthest forward location of 20-percent chord is a local characteristic produced by terminating the root of the strut in a kingpost for steering purposes; this can be simulated by a similar suspension. The elastic axes of subcavitating, semimonocoque struts and foils are expected to fall between 40- and 50-percent chord. It appears that some variation in GJ/EI may have to be accepted for some structures.

The ratio of the flutter speed of the prototype to that of the model can be determined by using the scaling principles described earlier which relate stiffness and flutter speed. For a given prototype, this ratio will depend on the model material. For one system studied, steel, titanium, and aluminum produced velocity scale ratios of 4.0, 2.1, and 1.5, respectively. Any of these materials would be suitable for studying flutter characteristics of a subcavitating hydrofoil system in a 50-knot test facility.

Model Size

Models must undergo flutter under flow conditions which produce forces similar to those experienced by prototype systems. The similarity of oscillatory forces for airfoil systems of different sizes can be approximated for values of Reynolds number R_n above 4×10^5, as indicated on page 710 of Bisplinghoff et al.[6] Hydrofoil prototypes have values of R_n far above this value, and models of practical size readily exceed it. For example, a 6-inch chord model at 14 knots has a value of $R_n = 10^6$.

TABLE 11 – COMPARISON OF PARAMETERS FOR SOLID CROSS SECTION MODELS AND FULL-SCALE STRUTS AND FOILS

Parameter	Range of Prototype Values	Value for NACA 16-Series Solid Section
Center of Gravity Location, x_{cg}/c	0.46–0.50	0.48
Elastic Axis Location, x_{ea}/c	0.20–0.60	0.48
GJ/EI	1.0–1.45	1.26 (aluminum) 1.49 (steel)
$\dfrac{4m \; (3/4 \; span)}{\pi \rho \, c^2}$	0.1–0.34	same*

*Using the following model materials and thickness-to-chord ratios:
  Aluminum, 4.1 to 13.4 percent thick,
  Titanium, 2.3 to 7.4 percent thick,
  Steel, 1.4 to 4.6 percent thick.

Experimental Configurations

All flutter models must be tested with sufficient sweepback to preclude divergence. Divergence speeds can be calculated with sufficient accuracy (as discussed elsewhere in this report) to make this possible. A sweep angle of 10 degrees is usually sufficient. Models with unswept struts common to full-scale craft will often diverge before experiencing flutter, but the prototype might achieve speeds closer to divergence and thereby undergo flutter. Extrapolation to smaller sweep angles should be made theoretically.

Models with load-bearing foils must operate well below the critical buckling load of the supporting strut. Vertical loading of near-buckling magnitude has decreased the speed at which predivergence deflections occurred.[8] Furthermore, load-bearing foils can cause bending deflections of a strut and make testing impossible even though divergence or buckling is not involved. Conventionally proportioned foils can readily produce excessive vertical loading on model struts because the model struts have relatively lower rigidity than prototype struts in order to simulate speeds above the prototype operating range. Therefore it is recommended that models permit control of vertical lift.

It is desirable to prepare pod and foil in additional configurations as well as in that corresponding to the prototype so that flutter can be obtained at lower speeds than for the configuration of interest. These will provide additional quantitative flutter boundaries to be used in combination with the theoretical projection. The additional results are particularly important if the prototype configuration does not undergo flutter within the speed range of the test facility. Failure of the prototype configuration to flutter within the 50-knot speed range of the high-speed towing basin at NSRDC[18] would normally correspond to a flutter speed for a similarly swept full-scale structure, well above speeds at which subcavitating flow can be maintained. Experimental results, shown in Figures 7 and 8 at $\mu_{torsion}$ = 1.1 demonstrate that large amounts of ventilation are destabilizing. The effect of moderate amounts of cavitation, such as would be expected during operation of a streamlined strut system in the vicinity of 60 knots, has not been investigated.

Experimental configurations should include several sweep angles above the divergence boundary. They should also include several depths because full-scale strut systems operate from zero to 100-percent submergence in rough water and cannot be considered to be limited to their design flying height. As previously discussed, existing data show that flutter speed changes with strut submergence.

---

[18]Brownell, W.F. and M.L. Miller, "Hydromechanics Cavitation Research Facilities and Techniques in Use at the David Taylor Model Basin," Symposium on Cavitation Research Facilities and Techniques, American Society of Mechanical Engineers (May 1964); also David Taylor Model Basin Report 1856 (Oct 1964).

40

During experimental work, care should be taken to accelerate the flutter model slowly and to increase speed in small increments. When damping is measured frequently, as can be done by using the rapid sweep excitation method described below, it is possible to investigate several speeds on a given test run.

Damping Measurement Techniques

The preferred method of testing flutter models consists of measuring, insofar as possible, the damping of the three lowest hydroelastic modes throughout the speed range below flutter. Knowledge of damping permits flutter—and thus the possibility of structural failure of the model—to be anticipated and assists in theoretical and practical understanding of the instability.

Three damping measurement techniques are available, but all are subject to limitations. The most versatile technique is rapid sweep excitation. A vibration generator is used to apply a sinusoidal force of rapidly varying frequency to a model. The frequency is swept from slightly below to slightly above a known resonance frequency. When the sweep is complete, the force is cut off. Damping values are obtained either from the decaying oscillation following excitation or from a phase plane plot of the frequency response function.[19] When the former method of analysis is used, this technique is not suitable for measuring damping above approximately 10 percent of critical damping.

A second, similar technique is known as line cut excitation. A line is attached to a model, pulled so as to deflect the model, and then cut. This method can produce a decay curve for a mode of oscillation having up to 10 percent of critical damping.

A third damping measurement technique involves measuring the mechanical impedance of a model at a resonance, thus giving the damping directly. A vibration generator and response pickup are required. This technique, which should be suitable for measuring high values of damping, requires long data acquisition times and has not been thoroughly evaluated for flutter work.

Damping measurement is hampered by the large range of damping values encountered for some struts as well as by the rather low frequencies of some hydroelastic modes. Hydroelastic modes of flutter models usually having damping ratios ζ of 5 percent or less at zero speed. This damping is due almost entirely to internal structural damping. The mode which

---

[19]White, R.G., "Use of Transient Excitation in the Dynamic Analysis of Structures," The Aeronautical Journal of the Royal Aeronautical Society Vol. 73, pp. 1047–1050 (Dec 1969).

is unstable in torsional flutter sometimes increases in damping only slightly before decreasing to zero at flutter inception. In this low damping region, rapid sweep excitation permits damping measurements to be made readily. The unstable mode in the bending flutter and transitional flutter regions, however, is very highly damped at intermediate speeds and drops rapidly to zero damping in a short speed range prior to flutter inception. This mode is difficult to detect prior to flutter, particularly because of its frequencies which are usually below 1 Hz. It might be possible to determine damping values for the bending flutter mode from mechanical impedance measurements.

The three excitation methods that have been demonstrated on full-scale systems—log impact, maneuvering, and crossing a wake—are similar to the line cut technique but have the additional limitation that deflection amplitude is uncontrolled at the present stage of development.

SUBCAVITATING FLUTTER THEORY

The accuracy of flutter speed predictions for struts with attached foils is, in general, unknown. The one theory evaluated to date shows only fair agreement with one experimental result. Predictions for simple struts and struts with pods have a known degree of inaccuracy, and this permits calculations to be corrected to give good flutter speed estimates for torsion-type struts.

Flutter Predictions for T-Foils

It is impossible to evaluate the accuracy of flutter predictions for subcavitating T-foils because insufficient flutter data are available for such systems. Only one flutter point exists, corresponding to the AGEH main T-foil. This result is used for a single-point evaluation of a modified strip flutter theory in the following discussion. In view of the wide variations in flutter speed and mode shape expected for practical T-foils, this evaluation is not of general applicability.

The previously mentioned full-scale and model data for the AGEH main T-foils constitute the available T-foil flutter data. The data are shown in terms of prototype values in Figure 9.

42

Among applicable flutter theories, only the modified strip flutter theory has been widely studied[1,20-22] and can be considered a possible candidate for design use. The theory employs a beam-lumped mass structural representation combined with two-dimensional strip loading modified for three-dimensional flow.[21] Figure 9 shows the hydroelastic mode characteristics of the AGEH system at 29-percent strut submergence as calculated by this theory. The calculation used the only stiffness data[23] and the most accurate inertial data[24] available. A slight simplification was introduced by using on each subdivision of the submerged portion of the structure constant steady loading values consisting of average three-dimensional values.

Flutter is predicted to occur in the second hydroelastic mode at a speed which is strongly dependent on the amount of structural damping. When the measured structural damping of the model is added to the calculated hydrodynamic damping, a flutter speed of 111 knots is obtained. All predictions above 50 knots, of course, are valid only in terms of scaled model speeds. The prediction, corresponding to the broken line of Figure 9, is 19-percent nonconservative with respect to the scaled model result of 93 knots. The solid lines indicate predictions for the prototype system based on measured structural damping of the prototype. The slightly higher prototype damping in Mode 2 raises the predicted flutter speed to 123 knots. This prediction cannot be compared with experiment because the slope of the damping curve is not known. The excellent agreement between predicted and measured damping at intermediate speeds indicates that the flutter mode is predicted accurately. This agreement does not imply that the theory can accurately predict damping, however, because the damping of other, less complex systems has not been accurately predicted at all speeds.[1,12]

The above comparison contains two known sources of inaccuracy:
1. The model torsional stiffness was lower than the prototype stiffness, as previously described, so that the prediction was apparently made for a more rigid system than the model.[23]

---

[20]Yates, E.C., Jr., "Flutter Prediction at Low Mass-Density Ratios with Application to the Finite-Span Noncavitating Hydrofoil," American Institute of Aeronautics and Astronautics Third Marine Systems and ASW Meeting (Apr–May 1968).

[21]Liu, Y.-N. and P.K. Besch, "Hydrofoil Flutter Analysis, Using a Modified Strip Theory," NSRDC Report 3624 (Jul 1971).

[22]Rowe, W.S. and T.G.B. Marvin, "A Program of Theoretical Research on Hydroelastic Stability," The Boeing Company, Contract N00014-67-C-0248 (Nov 1968).

[23]Clark, D.J., "Instrumentation and Static Calibration of the Foil Systems of the Navy Hydrofoil Boat PLAINVIEW (AG(EH)-1)," David Taylor Model Basin Report 2149 (Jan 1966).

[24]"AGEH-1 Weight Control Report–Final," Lockheed Shipbuilding and Construction Company (Jul 1969).

43

2. The straight beam structural representation was too simple for the strut system. Frequency predictions obtained by using a beam analogy have invariably given torsional frequencies that were too low for this system.[17,25]

Attempts to develop a constraint condition or parameter distribution which would improve the prediction without distorting the mode shape have been unsuccessful. However, a finite element analogy which represented both the forward and aft hinge points produced the desired improvement.[*] Therefore, struts similarly supported at multiple root points should be analyzed with finite element techniques. Flutter calculations have not been made with this method.

The importance of the above sources of inaccuracy could be determined by further analysis and possibly improve the prediction. However, the fact remains that only one data point is available for evaluation of the theory. It is concluded that the accuracy of flutter predictions for T-foils cannot be determined for the general case at present.

The above calculation illustrates the importance of structural damping measurements. If the prototype damping were 2 instead of 9 percent, the predicted flutter speed would be 83 knots, which is 40 knots or 33 percent lower than the present prediction. It is clear that damping must be accurately known if accurate predictions of torsional flutter are to be eventually obtained.

Flutter Predictions for Struts and Struts with Pods

Flutter speed predictions for torsion-type struts and struts with pods have a fairly well-defined relationship to experiment, based on a substantial number of comparisons. Although inaccurate in most cases, the magnitude and direction of inaccuracy correlate well with the mass ratio of the system. This correlation enables flutter speed to be estimated from the calculated value with greatly improved accuracy. A similar correction has not yet been determined for bending-type struts.

All available flutter speed predictions for struts without foils that employ the modified strip theory deviate from experiment in the manner shown in Figure 11. Struts with blunt-based profiles (included in Figure 11) do not exceed 5-percent thickness and are considered comparable to subcavitating struts. Predictions for bending-type struts ranged from 17 to

---

[25] Ransleben, G.E., Jr. and P.A. Cox, Jr., "Comparison of Measured Natural Frequencies of the One-Eighth Scale AG(EH) Flutter Model with Calculated Full-Scale Frequencies," Southwest Research Institute Project 02-2260, Contract N00600-68-D-0375 (Mar 1968).

[*] Private communication from R.E. Schauer, NSRDC Code 1966.
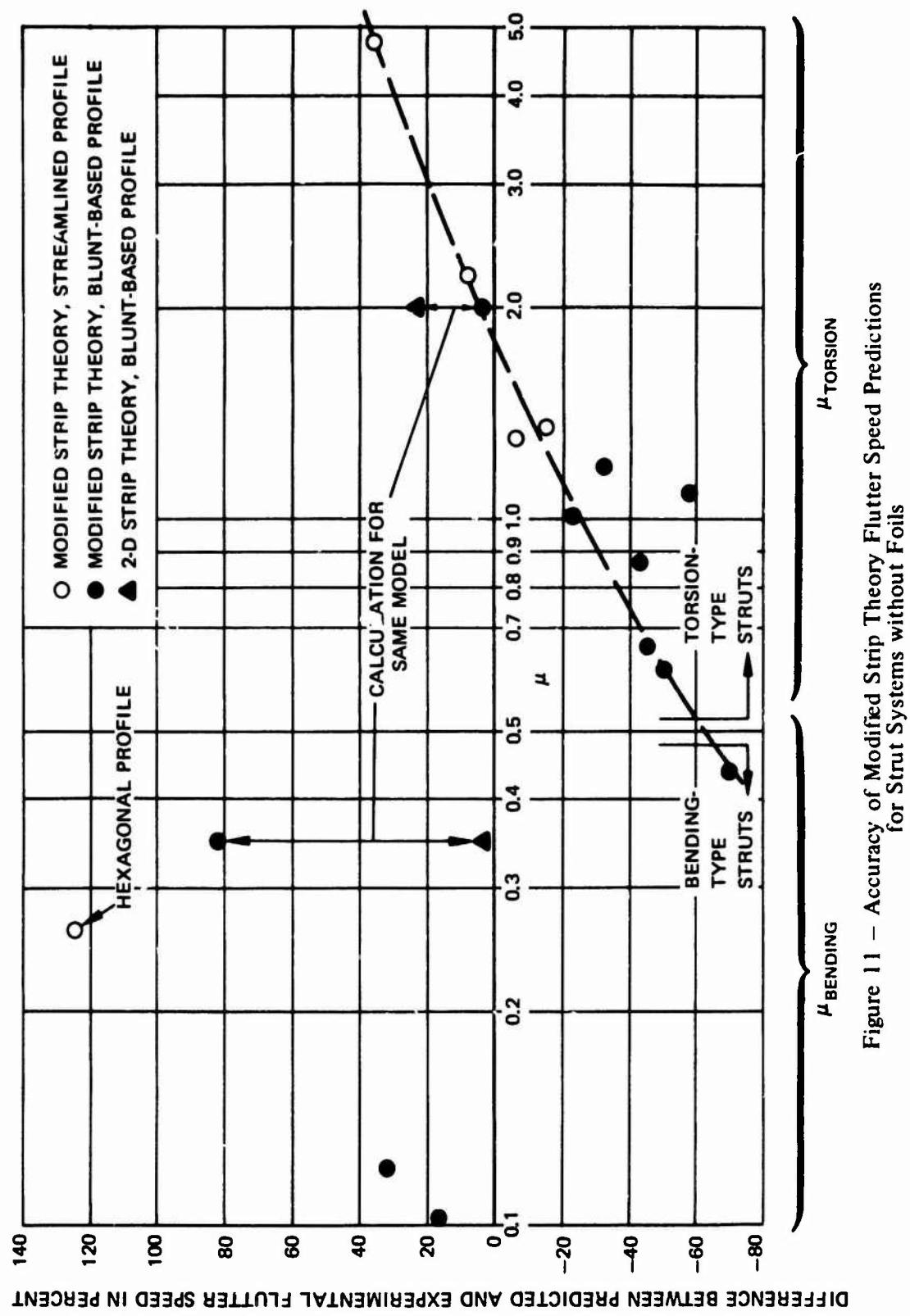
Figure 11 – Accuracy of Modified Strip Theory Flutter Speed Predictions
for Strut Systems without Foils

124 percent nonconservative, except for one result which was erroneously predicted as torsional flutter. These bending flutter boundaries correspond to a "new mode" instability and not to the instability which is erroneously predicted to occur in Mode 3.[1] Predictions for torsion-type struts varied from 59 percent conservative to 36 percent nonconservative, crossing over experimental values at approximately $\mu_{torsion}$ = 1.9. A dramatic shift in the direction of the deviation occurred when the flutter mode changed from bending to torsion.

The large number of comparisons for torsion-type struts makes it possible to derive a correction to calculated flutter speeds for that class of struts. Comparisons are too few to permit this to be done for bending-type struts. Since many additional data for bending-type struts are available, the necessary calculations should be carried out to determine whether a similar correction is feasible.

The calculated torsional flutter speed of a strut can be corrected as follows. First, the flutter mode of the strut must be determined to ensure that torsional flutter will occur. This can be done, as previously described, by examining the in-water mode shape of the second vibration mode of the strut. Second, the torsional mass ratio $\mu_{torsion}$ must be calculated for the strut. Finally, the approximate percentage correction can be obtained from the curve in Figure 11. It is important to note that pod hydrodynamics, represented by slender body theory (see page 417 in Bisplinghoff et al.[6]) must be included when using the suggested correction. It is not equivalent to use only the pod added mass.

Although bending flutter calculations cannot be corrected by using available data, it may be possible to obtain a more accurate prediction by using two-dimensional loading. Both the result shown in Figure 11 and independent calculations by Rowe and Marvin[22] for the strut at $\mu_{bending}$ = 0.101 and 0.262 showed great improvement when two-dimensional rather than three-dimensional loading was used. Further comparisons would be helpful in establishing this point.

The discrepancy between theory and experiment has been shown to lie in the hydrodynamic loading used.[22] The only suggested remedy has been to modify the calculated pressure distribution to account for possible cavitation patterns.[22] Such modifications strongly affected several flutter speed predictions in a favorable direction. However, a systematic approach is not available for determining the extent of cavitation. Cavitation is known to affect all profiles of practical thickness as speeds approach 50 knots. Comparisons of experimental and theoretical results at much lower speeds,[12] however, show that there are other sources of error in addition to cavitation. Improved accuracy will require improvements in hydrodynamic loading theory.

DIVERGENCE OF SUBCAVITATING STRUT SYSTEMS

KNOWN PARAMETER TRENDS

Vulnerable Systems

Both bending-type and torsion-type struts can diverge. Unswept bending-type struts probably do not flutter, and, therefore, divergence is expected to be the only mode of hydro-elastic instability for such struts.

Sweep Angle

Divergence speeds are strongly dependent on sweep angle. Calculations summarized by Abramson et al.[26] indicate that divergence will not usually occur above a sweep angle of 5 degrees. Divergence speed rapidly decreases as a strut is swept forward.

Elastic Axis Location

Divergence speed increases as the elastic axis is moved forward from a position aft of the aerodynamic center, and it becomes infinite when the elastic axis coincides with the aerodynamic center of the submerged lifting surface. Very accurate hydrodynamic characteristics must be used to calculate divergence speed for elastic axis locations near quarter chord.[12]

Submergence

Increasing the wetted area lowers the divergence speed of a surface-piercing strut or foil because the magnitude of the destabilizing hydrodynamic moment is increased. Therefore, divergence characteristics should be determined for the condition of maximum wetted area.

Size and Stiffness

For subcavitating systems with equal values of all nondimensional parameters, the divergence speeds of a model and a prototype are related as follows:

---

[26]Abramson, H.N. et al., "Hydroelasticity with Special Reference to Hydrofoil Craft," NSRDC Report 2557 (Sep 1967).

$$\frac{U_{D,\,prototype}}{U_{D,\,model}} = \frac{c^2_{model}}{c^2_{prototype}} \sqrt{\frac{EI_{prototype}\,\rho_{model}}{EI_{model}\,\rho_{prototype}}} \quad or \quad \frac{c^2_{model}}{c^2_{prototype}} \sqrt{\frac{GJ_{prototype}\,\rho_{model}}{GJ_{model}\,\rho_{prototype}}}$$

This relationship is the same as that for flutter speeds of model and prototype. Therefore, the flutter and divergence speeds bear the same relationship to each other in a scaled model as in its prototype. If a model encounters flutter prior to divergence, so will the prototype. If structural failure due to approaching divergence occurs prior to flutter, flutter of the prototype will not occur below the scaled speed reached by the model.

The above expression is valid for scaling both experimental and theoretical divergence boundaries when the theories use the same parameters. However, experimental results are generally limited in accuracy because models never attain their divergence speed. Instead, they fail at a lower speed which will generally not simulate the failure of the prototype.

Effect of Pods

Pods should lower the divergence speed of a strut. Theoretically (according to slender body theory), a pod exerts a pure, destabilizing couple on the tip of a strut without considering the attached strut or foils; see page 417 in Bisplinghoff et al.[6] No calculations of the magnitude of the effect have been made.

Effects of Foils

Foils should also lower the divergence speed of a strut. An attached foil is partially effective as a reflecting plate, thereby increasing the lift and moment on the strut. Similarly, the presence of a yawed strut has been shown to affect the loading on an attached foil.[27] No divergence calculations which consider this interaction are available.

---

[27]French, H., "Hydrofoil Patrol Craft PC(H) Fwd Hydrofoil Vibration Modes," The Boeing Company, Aerospace Division, Bureau of Ships Plan PC(H) – 1 518 1993317 (Oct 1961).

48

IMPLICATIONS FOR PROTOTYPE SYSTEMS

Several design families of T-foils, based on existing T-foil structures, are free from divergence or undesirable static deflections in subcavitating flow within the size range of existing craft. Model experimental results support the use of modified strip theory calculations for predicting divergence characteristics.

AGEH Main Design Family

Divergence information for the design family based on the AGEH main T-foil is provided by the previously described flutter test of the 1/8-scale AGEH model. Since no instability occurred prior to a model speed of 33 knots, the full-scale system has a divergence speed above 93 knots under subcavitating conditions. Therefore, the full-scale main T-foil system will experience no undesirable deflections up to a speed of 50 knots. All geometrically similar systems will also be free from static deflections. Parameters for the existing full-scale system are given in Tables 7 and 8.

Other Design Families

Other operational T-foils have been free from the large deflections which precede divergence. Therefore those existing T-foils define acceptable design families comprised of geometrically similar systems. System parameters for three additional such systems are summarized in Tables 7 and 8. Possible structural differences in very large struts limit the applicability of these design families to systems no larger than the AGEH main T-foil.

Validity of Divergence Calculations

Calculations of divergence characteristics using modified strip theory are expected to give accurate design information. Confidence in the theory is based on two studies of strut divergence behavior which gave excellent agreement between theory and experiment.[12,28]

---

[28]Caspar, J.R., "Divergence Analysis of Swept Hydrofoils—Computer Program (SWDIVRG)," NSRDC Report 4245 (Apr 1974).

The strut models included a streamlined profile model and a thin, blunt-based profile model. Both studies analyzed model divergence characteristics from the standpoint of the large deflections or stress levels that precede divergence. Excessive deflections occurred at speeds ranging from 33 to 93 percent of accurately predicted divergence speeds. However, excessive deflections at small fractions of the divergence speed occurred only when higher modes appeared in the solution. When only the fundamental bending and torsion modes were involved, an operating limit of 60 percent of the divergence speed was adequate. The anomalous behavior can be detected by checking the mode shapes and deflection magnitudes as functions of speed.

These results indicate that lifting-surface structures must be restricted to speeds far below their divergence speeds. Restrictions must be based on avoiding unacceptable deflections and stress levels for particular structural systems.

DIVERGENCE THEORY

Convenient divergence analysis procedures have recently been developed by Caspar.[28] A computer program is now available which performs divergence calculations for any lifting-surface structure. A formula is given for direct calculation of divergence speed for uniform cantilever struts or foils.

The computer program presented by Caspar[28] is based on a strip loading theory that has been modified for three-dimensional flow and combined with a lumped parameter structural representation. The loading must be supplied separately by the user from a lifting surface theory or obtained from curves provided. The structural analogy for other than uniform cantilever struts must be obtained from the SADSAM V structural analysis program[29] or its equivalent. In addition to deflections, the program outputs include bending and torsional moments which can be used to determine stress levels for cantilever beam constraint conditions.

MODEL EXPERIMENTS

It does not appear productive to use model experiments to determine divergence speeds of structures. Divergence theory will be sufficiently accurate in most cases, and models

---

[29]Peterson, L., "Theoretical Basis for SADSAM Computer Program," MacNeal-Schwendler Corporation Project Report (Dec 1970).

permit only approximations to be obtained because of their predivergence failure. If experiments are performed, however, provisions should be made for producing small static deflections of the structure so that a flow-induced deflection boundary can be obtained. An excitation technique for this purpose is described by Besch and Liu.[12] Further experimental experience in divergence testing is described by Hilborne[1] and by Squires.[9] The "load boundaries" encountered by Squires are correlated with divergence speeds by Caspar.[28]

FLUTTER OF CAVITATING STRUT SYSTEMS

Cavitation and ventilation lower the flutter speed of at least some lifting surfaces. When the higher speeds associated with cavitation are taken into account, cavitating and ventilated systems are potentially much more susceptible to flutter instability than are subcavitating systems.

This section discusses the differences between the flutter of cavitating and ventilated systems and that of subcavitating systems. These differences consist of changes in flutter speed produced by ventilation and the need for an additional nondimensional parameter when flutter boundaries are scaled in the presence of cavitation and ventilation.

Also discussed are the design implications of T-foil models and a prototype system. Design guidance is available from the prototype system up to a speed of 62 knots.

THREE TYPES OF CAVITIES

Cavitation is a local flow condition which affects the hydrodynamic loading on a surface. Three types of cavities occur in operating hydrofoil systems: vapor cavitation, natural ventilation, and artificial ventilation. Vapor cavitation refers to submerged cavities in which the pressure is near that of water vapor. Natural ventilation occurs when cavities are filled with air at atmospheric pressure, usually because the cavity is directly connected to the atmosphere. Artificial ventilation corresponds to cavities into which air is injected.

Parameters which determine the occurrence and distribution of cavitation and ventilation are the geometry of the surface in contact with the flow and flow conditions. Nondimensionally, the system shape, cavitation number σ_c, and Froude number F_n describe system cavitation characteristics. Comparatively speaking, vapor cavitation corresponds to high values of σ_c, artifical ventilation to intermediate values, and natural ventilation to low values. These variations in σ_c lead to different scaling laws for each of the three types of cavitation.

51

KNOWN PARAMETER TRENDS

Lifting-Surface Profile

Certain cavitation patterns have destabilizing effects on lifting surfaces, and profiles which produce these cavitation patterns should be viewed with special caution. Specifically, lifting surfaces can be greatly destabilized by long cavities which separate from the leading edge on one or both sides of the surface. Stability increases as the separation point of a long cavity on one side of a section moves aft from the leading edge to 10 percent of the chord.

At moderate speeds, these cavitation patterns would be produced by square-nosed profiles, by profiles with a spoiler, and by sharp-nosed profiles at sufficiently large angles of attack. At high speeds (above 50 knots), all profiles will cavitate aft of the leading edge even at small angles of attack, although cavity lengths might be less than 1 chord. Since nonzero incidence angles are unavoidable due to sea conditions, maneuvering, or structural oscillation, lifting surfaces operating at high speeds will experience flow conditions which are similar to those known to be destabilizing. For this reason, all reliable simulations of high-speed systems must model the cavitating flow conditions; stability estimates based on fully wetted systems might be unconservative.

The destabilizing effect of cavitation was observed on a surface-piercing strut[1] and on a two-dimensional hydrofoil.[30,31] The surface-piercing strut data shown in Figures 7 and 8 exhibited a decrease of 35 percent in flutter speed when a blunt-based profile was changed to a blunt-nosed profile at a model speed high enough to produce a long cavity. A two-dimensional wedge-shaped hydrofoil had a flutter speed as much as 34 percent lower when a long rather than a short (1/2-chord) cavity separated from the leading edge.[30] There was little difference in flutter speed between a wedge foil with a short, vapor cavity[30] and a streamlined foil.[31] This suggests that only long cavities have a destabilizing effect, at least for some foils. Increases in stability as the cavity separation point moves aft from the leading edge have been both calculated and observed for two-dimensional hydrofoils.[32]

---

[30]Besch, P.K., "Flutter and Cavity-Induced Oscillation of a Two-Degree-of-Freedom Hydrofoil in Two-Dimensional Cavitating Flow," NSRDC Report 3000 (Apr 1969).

[31]Cieslowski, D.S. and P.K. Besch, "Flutter of a Two-Degree-of-Freedom Hydrofoil in Two-Dimensional Subcavitating Flow," NSRDC Report 3183 (Jan 1970).

[32]Song, C.S., "Flutter of Supercavitating Hydrofoils–Comparison of Theory and Experiment," Journal of Ship Research, Vol. 16, No. 3, pp. 153–166 (Sep 1972).

Size and Stiffness

The characteristics of a cavitating or ventilated flutter model have a known relationship to flutter characteristics of prototype systems of different sizes. Unlike subcavitating prototypes, however, cavitating prototypes generally cannot be of arbitrary stiffness. In some cases at least, the stiffnesses EI and GJ of the prototype must bear specific relationships to the stiffnesses of the model. This restriction is created by the need to maintain equal values of cavitation number σ_c at equivalent depths of model and prototype. Velocity and size scaling laws are given below for each type of cavitation, along with related stiffness requirements.

Prototype and model flutter speeds and stiffnesses must satisfy the following general relationships for all types of cavitation:

$$\frac{U_{f, \text{prototype}}}{U_{f, \text{model}}} = \frac{c^2_{\text{model}}}{c^2_{\text{prototype}}} \sqrt{\frac{EI_{\text{prototype}} \rho_{\text{model}}}{EI_{\text{model}} \rho_{\text{prototype}}}} \quad \text{or} \quad \frac{c^2_{\text{model}}}{c^2_{\text{prototype}}} \sqrt{\frac{GJ_{\text{prototype}} \rho_{\text{model}}}{GJ_{\text{model}} \rho_{\text{prototype}}}}$$

with the requirement that

$$EI_{\text{prototype}} = \frac{c^4_{\text{prototype}} (p_a + \rho gh - p_c)_{\text{prototype}}}{c^4_{\text{model}} (p_a + \rho gh - p_c)_{\text{model}}} EI_{\text{model}}$$

$$GJ_{\text{prototype}} = \frac{c^4_{\text{prototype}} (p_a + \rho gh - p_c)_{\text{prototype}}}{c^4_{\text{model}} (p_a + \rho gh - p_c)_{\text{model}}} GJ_{\text{model}}$$

For some types of cavitation, these relationships can be simplified in the following manner.

Vapor Cavitation. Vapor cavities have no air inflow; cavity pressures p_c are very low, only slightly above the pressure of water vapor (0.4 psi). When both model and prototype operate beneath an atmospheric pressure of 14.7 psi at depths much less than 34 ft (corresponding to a pressure head much less than atmospheric pressure), the stiffness relationships become

$$EI_{\text{prototype}} \cong \frac{c^4_{\text{prototype}}}{c^4_{\text{model}}} EI_{\text{model}}$$

53

$$GJ_{prototype} \cong \frac{c^4_{prototype}}{c^4_{model}} \; GJ_{model}$$

Under these conditions, the flutter speeds of model and prototype are approximately equal.

$$\frac{U_{f, prototype}}{U_{f, model}} \cong \sqrt{\sqrt{\frac{\rho_{model}}{\rho_{prototype}}}} \cong 1.0$$

Natural Ventilation. Naturally ventilated cavities are defined as having a cavity pressure p_c equal to atmospheric pressure. This will occur for cavities with a wide opening to the atmosphere. When $p_c = p_a$, stiffness relationships become

$$EI_{prototype} = \frac{c^5_{prototype}}{c^5_{model}} \; EI_{model}$$

$$GJ_{prototype} = \frac{c^5_{prototype}}{c^5_{model}} \; GJ_{model}$$

The resulting flutter speed ratio is

$$\frac{U_{f, prototype}}{U_{f, model}} = \sqrt{\frac{\rho_{model} \, c_{prototype}}{\rho_{prototype} \, c_{model}}} \cong \sqrt{\frac{c_{prototype}}{c_{model}}}$$

High speeds and restricted air paths result in cavity pressures below atmospheric pressure. Such cavity conditions must be treated in the same manner as artificially ventilated cavities.

Artificial Ventilation. Artificially ventilated cavities have a wide range of cavity pressure values, depending on the air flow rate and other conditions. The general scaling relationships given above must be used to account for these wide pressure variations.

54

In addition to the above categories, combinations of two or three types of cavitation can occur. Such cases would have to be scaled approximately according to the cavitation considered most important. This is expected to be the type of cavitation that covers the largest area on the system lifting surfaces.

Under certain cavitation conditions, it is probable that the above scaling laws need not be fulfilled and that subcavitating scaling can be used. An example is the existence of cavities much longer than 1 chord; a change in cavity length (cavitation number) has little effect on hydrodynamic loading. When the loading is independent of cavitation number, the latter can be neglected and the above restrictions on stiffness are not needed.

Effects of Foils

A thin, blunt-based profile strut-pod system can either be stabilized or destabilized by the addition of a relatively large, lightweight foil. A foil is believed to change the generalized mass ratio of the strut system. The resulting flutter speed changes may be qualitatively similar to the curve in Figure 5.

Huang[8] found that when a foil was added, the flutter speed of a naturally ventilated strut-pod system could increase as much as 75 percent or decrease by as much as 18 percent as a function of strut submergence ℓ. These data are not considered quantitatively reliable for scaling purposes because the strut was near a buckling condition. Because the strut had a thickness of only 3.6 percent, these trends are probably accurate for subcavitating struts as well.

IMPLICATIONS FOR PROTOTYPE SYSTEMS

Much less design information is available for cavitating T-foils than for fully wetted T-foils. Only one cavitating T-foil design family is available for design guidance, and this is limited to a known stable speed of 62 knots. Other cavitating designs are stable to higher speeds but have not been operated as full-sized prototypes. These results are discussed below.

DENISON Tail Design Family

The DENISON tail T-foil,[4] partially described in Tables 12 and 13, defines a design family of geometrically scaled T-foils which are known to be stable up to a speed of 62 knots.

TABLE 12 – DIMENSIONED PARAMETERS FOR FULL-SCALE AND MODEL T-FOILS WITH BLUNT-BASED STRUT PROFILES

Strut	FRESH-1 1/4-Scale Transiting Tail	FRESH-1 1/4-Scale Transiting Main	FRESH-1 Demonstration Outboard	FRESH-1 Demonstration Centerline	DENISON Tail
L, in.	35.7	28.8	113	113	261.8
c (3/4 span) in.	5.84	7.5	28.8	28.8	94
Λ (1/4 chord), deg	9	9	8.0	8.0	0.0
x_{ea} (3/4 span), in.	4.4	6.0	Not available	Not available	Not available
x_{cg} (3/4 span), in.	2.66	3.06			
m (3/4 span), lb/in.	0.402	0.491			
I_{my} (3/4 span), lb-in.	2.40	9.68			
EI (3/4 span), lb-in.^{2}	2.4×10^6	4.3×10^6			
GJ (3/4 span), lb-in.^{2}	2.3×10^6	5.1×10^6	Not available	Not available	Not available
Profile	Blunt based	Blunt based	Parabolic	Parabolic	Blunt based
Thickness (3/4 span)	20 percent	16 percent	11 percent	11 percent	7.5 percent
Dihedral Angle, deg	0.0	10	Not available	0.0	0.0
Pod					
Length, in.	16.6	22.1	29.1	44	226
Max . Diameter, in.	1.3	2.0	Not available	Not available	30
x_{nose}, in.	5.5	10	0.0	15	0.0
x_{cg}, in.	7.9	11	Not available	Not available	Not available
M, lb	1.2	2.2	Not available	Not available	6,000
I_y, lb-in.^{2}	39.5*	10*	Not available	Not available	Not available

TABLE 12 (Continued)

Foil	FRESH-1 1/4-Scale Transiting Tail	FRESH-1 1/4-Scale Transiting Main	FRESH-1 Demonstration Outboard	FRESH-1 Demonstration Centerline	DENISON Tail
Area, ft^2	0.385	0.864	7.46	7.46	49.4
Root Chord, in.	9.2	13.7	29.1	29.1	82
Tip Chord, in.	0.87	1.3	8.73	8.73	31
Full Span, in.	11.1	16.6	56.8	56.8	126
Λ, deg	48.4	48.4	18.0	18.0	11.4
x_{foil}, in.	4.5	2.75	2	2	−13
M, lb	3.16	10.9	Not available	Not available	Not available
x_{cg}, in.	8.9	11.8	Not available	Not available	Not available
Profile	NACA 16-X04.1 x = 0.171 a = 1.0	NACA 16-X04.1 x = 0.171 a = 1.0	Parabolic cambered	Parabolic cambered	NACA 16-X04 x = 0.55 a = 1.0
Flutter Condition					
ℓ, in.	3.9	11.6	Not available	Not available	57.5 to 146.5
U_f, knots	89**	94***	above 80	above 80	above 62
f_f, Hz	17.0**	7.5***	Not available	Not available	Not available
Mode Shape	Uncertain	Uncertain	Not available	Not available	Not available
˙	0.10	0.06	Not available	Not available	Not available
Divergence Condition					
ℓ, in.	6.6	18.9	Not available	Not available	Not available
U_D, knots	98.5	80	above 80	above 80	above 62

*About vertical axis through strut center of gravity.

**Minimum flutter speed encountered; foil angle of attack was 3 deg.

***Minimum flutter speed encountered; foil angle of attack was 2 deg.

TABLE 13 – NONDIMENSIONAL PARAMETERS FOR FULL-SCALE AND MODEL T-FOILS WITH BLUNT-BASED STRUT PROFILES

Strut	FRESH-1 1/4-Scale Transiting Tail	FRESH-1 1/4-Scale Transiting Main	FRESH-1 Demonstration Outboard	FRESH-1 Demonstration Centerline	DENISON Tail
L/c	6.11	3.84	3.92	3.92	2.79
AR (to keel)	3.10	2.40	2.77	2.62	1.52
κ	0.026	0.041	0.036	0.036	0.0
x_{ea} (3/4 span)/c	0.80	0.80	Not available	Not availa	Not available
x_{cg} (3/4 span)/c	0.49	0.41	Not available	Not available	Not available
$4m$ (3/4 span)/$\pi \rho c^2$	0.479	0.308	Not available	Not available	Not available
$16 I_{my}$ (3/4 span)/$\pi \rho c^4$	0.291	0.436	Not available	Not available	Not available
Pod					
Fineness Ratio	12.8:1	11.1:1	Not available	Not available	7.5:1
Diameter/c	0.223	0.267	Not available	Not available	0.319
x_{nose}/c	0.942	1.33	0.0	0.521	0.0
$x_{cg,pod}/c$	1.35	1.47	Not available	Not available	Not available
M_{pod}/M_{strut}	0.065	0.119	Not available	Not available	above 0.52
I_{pod}/I_{strut}	0.164	0.360	Not available	Not available	Not available
Foil					
c_{root}/c	1.69	1.83	1.0	1.0	0.87
AR	2.20	2.20	3.0	3.0	2.23
Λ, deg	48.4	48.4	18.0	18.0	11.4
τ	0.0952	0.0950	0.30	0.30	0.38
x_{foil}/c	0.77	0.37	0.069	0.069	−0.14
x_{cg}/c	1.52	1.57	Not available	Not available	Not available
M_{foil}/M_{strut}	0.168	0.602	Not available	Not available	Not available

TABLE 13 (Continued)

Flutt- Condition	FRESH-1 1/4-Scale Transiting Tail	FRESH-1 1/4-Scale Transiting Main	FRESH-1 Demonstration Outboard	FRESH-1 Demonstration Centerline	DENISON Tail
AR (strut wetted area)	0.69	1.51	0.80	0.73	Not available
k_{nf}	0.17	0.093	Not available	Not available	Not available
$4\,EI\,(3/4\,span)/\pi\rho\,c^2\,\omega_f^2\,L^4$	4.2×10^{-3}	5.6×10^{-2}	Not available	Not available	Not available
$16\,GJ\,(3/4\,span)/\pi\rho\,L^2\,\omega_f^2\,c^4$	0.73	3.9	Not available	Not available	Not available
R_{nf} (3/4 span)	6.0×10^6	8.1×10^6	above 2.7×10^7	above 2.7×10^7	above 5.6×10^7
F_{nf}	38	35	above 15	above 15	above 5.3
σ_f (at surface)	0.092	0.083	below 0.11	below 0.11	below 0.19
Divergence Condition					
AR (strut wetted area)	1.16	2.40	0.80	0.73	Not available
$EI\,(3/4\,span)/2\,\pi\rho\,U_D^2\,L^4$	6.4×10^{-4}	4.1×10^{-3}	Not available	Not available	Not available
$4\,GJ\,(3/4\,span)/2\,\pi\rho\,U_D^2\,c^2\,L^2$	0.11	0.29	Not available	Not available	Not available
R_{nD} (3/4 span)	6.7×10^6	6.9×10^6	above 2.7×10^7	above 2.7×10^7	above 5.6×10^7
F_{nD}	42	30	above 15	above 15	above 5.3
σ_D (at surface)	0.075	0.11	below 0.11	below 0.11	below 0.19

As previously described, all members of a design family have components (skins, ribs, spars, etc) that are geometrically scaled from the parent and material properties equal to those of the parent. This family should not be extrapolated to larger systems without considering possible structural differences.

FRESH-I Transiting T-Foils

Quarter-scale flutter models of the FRESH-I transiting main and tail T-foils were tested by Mitchell and Rauch[2] in order to determine the flutter speeds of the prototype systems. The transiting T-foils were constructed in 1963 as a second-generation set of foils for FRESH-I, but these have never been used on the craft. Model parameters are listed in Tables 12 and 13. Judging by the low reduced frequencies of flutter, both T-foils experienced bending flutter.

The model flutter results can be scaled to the size of both the FRESH-I prototype and larger prototypes. Cavitation on the models consisted of vapor cavitation on the foils and natural ventilation aft of the blunt-based struts, although cavity pressure may have been below atmospheric at the high speed involved. Although cavitation number σ would not be preserved for systems of different sizes, the cavities were long and therefore loading would be insensitive to differences in σ. No observations were reported of cavitation separating from the leading edge of the struts. Since cavitation number can be neglected, it is possible to scale flutter speeds to systems of different size and arbitrary stiffness by using subcavitating scaling relationships.

The full-scale transiting systems are geometrically identical in all parts and material to the models, and therefore their stiffnesses are higher by the fourth power of the length ratio. This relationship yields equal flutter speeds for model and full-scale systems since the models were tested in seawater. The full-scale main and tail systems are therefore expected to flutter at 94 and 89 knots, respectively.

Scaling these model results to larger prototypes than the FRESH-I systems requires knowledge of prototype stiffnesses. It is unlikely that large prototypes geometrically similar to the transiting systems would be built because such prototypes would be more rigid than any of the other systems shown in Figure 10. The PCH-PHM design is the most rigid design yet produced for craft above 100 tons, and it probably represents a practical maximum for stiffness.

The bending stiffness of the PCH strut gives flutter speeds of 82 and 63 knots, for T-foils similar to the FRESH-I transiting main and tail systems, respectively. This result applies to systems on craft of 100- to 200-ton displacements. It is not known whether larger designs could maintain this degree of stiffness.

60

These projections along with the divergence speed projections described in another section indicate that the FRESH-1 transiting T-foil designs are not acceptable for full-sized operational craft at speeds near 80 knots. It is not clear which parameters are responsible for this degree of instability. Structurally, the transiting systems differ from subcavitating T-foils most markedly in their tapered struts and, according to the description given by Squires,[33] in the far aft location of the elastic axis at 80 percent of the chord.

FRESH-1 Demonstration T-Foils

Two additional T-foil designs, the FRESH-1 demonstration outboard and centerline T-foils, have been operated successfully under cavitating conditions. However, these T-foils may be of only limited use for design guidance. An incomplete list of parameters for these foils is included in Tables 12 and 13. The FRESH-1 demonstration foils are stable to at least 80 knots, but they are small in size. If these foil systems are extraordinarily rigid, in the manner of the transiting foils, and geometric scaling to larger sizes is impractical, reduced stiffnesses may lower the known stable speed to below 80 knots.

EXPERIMENTAL MODELING TECHNIQUES

Stringent demands are placed on model design and experimentation by the need to preserve cavitation number. Fortunately, cavitation number must be preserved for accurate simulation only when cavitation or ventilation covers part of a foil surface or extends only a short distance beyond the surface. In such cases, the model must be tested in a variable-pressure facility. Very high speeds at reduced pressures can be produced only in the 36-inch water tunnel at NSRDC,[18] where a free surface cannot be properly modeled. Model design must yield an exact profile and stiffness; in most cases, this cannot be accomplished with a solid cross section model but requires a complex model design.

When hydrodynamic loading is largely independent of cavitation number, only the pattern of cavitation on the prototype has to be produced on the model. This permits modeling to be carried out by using the same approaches as for subcavitating systems, except that sufficient speed must be attained to produce the required cavitation.

---

[33]Squires, C.F., Jr., "Preliminary Flutter Analysis of the Design M-51 Hydrofoil Craft (FRESH 1)," Grumman Aircraft Engineering Corporation Report DA M51-478.1 (Mar 1963).

CAVITATING FLUTTER THEORY

Flutter theory for cavitating systems in three-dimensional flow is rudimentary at present. Development has been held back not only by the limited amount of data obtained from realistic T-foil systems – the FRESH-I transiting systems[2] are the only such systems for which data are available – but also by the lack of unsteady hydrodynamic theory for all but two cavitation patterns. These cavitation patterns are short cavities separating from the leading edge of a foil[34] and long cavities separating from a foil at an arbitrary distance aft of the leading edge.[35] No flutter analyses have been performed for realistic structures subject to these cavitation patterns. No theory is available for the many other cavitation patterns expected on practical systems, such as blunt-based profiles at high speeds.

There are many indications that subcavitating load theory is not suitable for predicting flutter speeds of cavitating strut systems other than torsion-type struts with thin, blunt-based profiles. Rowe and Marvin[22] demonstrated that calculated flutter speeds are extremely sensitive to pressure distribution changes which simulate cavitation (and to no other parameter). Flutter predictions for a strut which probably cavitated at several locations along its chord were much more nonconservative than predictions for other cavitating profiles,[1,21,22] as shown at $\mu_{bending} = 0.262$ in Figure 11. Squires obtained "poor" correlation between theory and experiment when using subcavitating load theory to predict flutter characteristics of cavitating T-foils.[33] The lift slope of a 24-percent-thick, blunt-based profile strut was found to be substantially higher than that of a streamlined strut of 12-percent thickness,* suggesting that different modifications to a strip theory would be required for a moderately thick blunt-based strut and a streamlined strut.

The semiempirical approach provides an alternative to pure theory. This approach would involve measurement of the unsteady lift and moment on a model system in properly simulated flow. The measured loading would be used with a suitable structural representation to calculate flutter speeds. The accuracy of this method depends on the accuracy of the measured loading. Considerable expense would be involved in obtaining spanwise distributions of loading.[36] Because the expense of an accurate measurement of load distribution

---

[34]Steinberg, H. and S. Karp, "Unsteady Flow Past Partially Cavitated Hydrofoils," Proceedings Fourth Naval Hydrodynamics Symposium (Aug 1962).

[35]Kaplan, P. and C.J. Henry, "A Study of the Hydroelastic Instabilities of Supercavitating Hydrofoils," Journal of Ship Research, Vol. 4, No. 3, pp. 28–38 (Dec 1960).

[36]Ransleben, G.E., Jr., "Experimental Determination of Steady and Unsteady Loads on a Surface Piercing, Ventilated Hydrofoil," Journal of Ship Research, Vol. 13, No. 1, pp. 1–11 (Mar 1969).

*Reported by N.L. Dailey in an NSRDC report for internal use.

would probably be greater than the expense of building an elastically scaled model which could be used to establish flutter stability directly, the semiempirical approach is of practical use only when it is desired to avoid building a large number of flutter models.

It is concluded that cavitating flutter theory is not now available for general design use. Based on results in Figure 11, torsion-type struts with thin, blunt-based profiles can be treated by using subcavitating flutter theory.

DIVERGENCE OF CAVITATING STRUT SYSTEMS

Relatively little information on the divergence of cavitating systems is available for design use. Because of the drastic changes in hydrodynamic loading which accompany cavitation, cavitating systems should have divergence characteristics which are substantially different from those of subcavitating systems. Design is hindered by the lack of theories of established accuracy, leaving model experiments as the only dependable alternative.

KNOWN PARAMETER TRENDS

Sweep Angle

The effect of sweep angle in raising divergence speed has been experimentally demonstrated for thin, blunt-based struts by Hilborne[7] and by Squires.[9] Struts at less than 5 degrees of sweep experienced large deflections and occasional yielding, which were indicative of approaching divergence, while deflections were insignificant as higher sweep angles. Flutter replaced divergence as the mode of hydroelastic instability at sweep angles of 5 degrees and higher.

Size and Stiffness

Divergence speeds of cavitating systems scale the same as flutter speeds of cavitating systems. In some cases, the requirement to preserve cavitation number places restrictions on model stiffness.

63

IMPLICATIONS FOR PROTOTYPE SYSTEMS

The DENISON tail T-foil,[5] described in Tables 12 and 13, establishes a design family of geometrically scaled, equivalent material systems which are free from divergence-related deflections up to a speed of 62 knots. Extrapolations should not be made to larger size systems without further study.

Two additional cavitating T-foil designs have been found to be subject to large predivergence deflections, in one case at a speed below flutter inception. The designs are the 1/4-scale FRESH-I transiting main and tail T-foils,[2] parameters for which are given in Tables 12 and 13. Since both systems were capable of operation at speeds above the initially unstable speeds, the flow presumably changed in some way at the higher speeds. It is therefore obviously important to establish stability for all possible operating conditions, not merely the highest speed.

According to the scaling approach explained earlier for flutter speeds, predivergence deflections will occur on the full-scale FRESH-I transiting main and tail T-foils at 80 and 98.5 knots, respectively, the same speeds as for the models. Larger scale prototypes of both the main and tail systems, with stiffnesses corresponding to the PCH-PHM design family shown in Figure 10, would be affected at 70 knots. These designs could not be used with confidence at speeds very far into the cavitating flow region.

Prototype systems should not be expected to survive a static instability in the manner that the transiting system models did. This result is unique among experimental results; most other instability-related deflections have caused model failure and no other instances have been successfully pursued to higher speeds. The least indication of instability in a design would of course not be tolerable. Although it is assumed that changes in loading due to varying amounts of cavitation led to survival of the transiting models, other changes, e.g., structural, could have occurred.

CAVITATING DIVERGENCE THEORY

Divergence theory for cavitating systems is unavailable for design use because flutter theory of cavitating systems is deficient except for thin, blunt-based profile struts. The semiempirical approach mentioned in discussing cavitating flutter theory is a possible approach for divergence predictions as well.

MODEL EXPERIMENTS

Either solid-section or more complex models could be used to establish divergence-free speed ranges of prototypes. Care must be taken to simulate the prototype cavitation pattern exactly in those cases where loading will be sensitive to changes in cavity length. Cavitation produced by operational angles of attack must be considered in the model study.

CONCLUSIONS

1. Within the size range of existing hydrofoil craft, several design families of T-foils are free of flutter and divergence at all subcavitating speeds or up to approximately 50 knots.

2. Within the size range of existing craft, one design family of T-foils is stable in the cavitating speed range up to a speed of 62 knots. No stable designs have been established above 62 knots.

RECOMMENDATIONS

1. The engineering aspects of constructing T-foil systems larger than the AGEH main T-foil should be studied to determine the impact of possible structural differences on hydro-elastic stability and other design criteria.

2. Studies of flutter and divergence characteristics should be made for both subcavitating and cavitating T-foils. Model testing and theoretical analysis should be used.

3. A technique for measuring damping of full-scale T-foils should be developed and should include installation and trial on an existing craft. The technique should then be used on all future craft.

4. A standard specification should be developed for hydroelastic stability on high-speed craft.

ACKNOWLEDGMENTS

APPENDIX

KINEMATIC SCALING OF FLUTTER AND DIVERGENCE OF T-FOILS

Principles of dimensional analysis permit flutter data from one T-foil to be used to predict flutter characteristics of other T-foils of different size and stiffness. Flutter boundaries of a prototype and its model can be compared if the two systems undergo equivalent motions, corresponding to zero damping, when all scaling relationships are satisfied. This condition is called kinematic similarity or scaling.[37] It occurs when the ratios of displacement, velocity, and acceleration between the two systems are the same at all points.[38]

Scaled systems have equal values or effectively equal values of all nondimensional parameters. The required nondimensional parameters for kinematic scaling can be obtained either by nondimensionalizing the equations of motion of the system, as has been done for a wing (see the material starting on page 699 in Bisplinghoff et al.[6]) or by forming dimensionless ratios of all parameters that should appear in those equations.

This treatment will list the relevant parameters and the dimensionless ratios obtained from an unpublished nondimensionalization of the equations of motion. Some parameter ratios are based on structural properties at the 3/4-span position. These properties are representative of the overall properties of tapered structures (see page 533 in Bisplinghoff et al.[6]).

SUBCAVITATING FLUTTER

Dimensioned Flutter Parameters for Subcavitating T-Foils

Strut Parameters: L, c, $L \cos \Lambda$, $x_{ea}(y)$, $x_{cg}(y)$, $m(y)$, $I_{my}(y)$, $EI(y)$, $GJ(y)$, ℓ

Pod Parameters: length, maximum diameter, x_{nose}, x_{cg}, M, I_y, I_ϕ

Foil Parameters: L, $c(z')$, $L \cos \Lambda$, x_{foil}, $x_{ea}(z')$, $x_{cg}(z')$, $m(z')$, I_y, $I_{mz'}(z')$, I_ϕ, $EI(z')$, $GJ(z')$

System Parameters: ρ, c_s (in air)

---

[37]Langhaar, H.L., "Dimensional Analysis and Theory of Models," John Wiley & Sons, Inc., New York (1951).

[38]Albertson, M.L. et al., "Fluid Mechanics for Engineers," Prentice-Hall, Inc., Englewood Cliffs, N.J. (1960).

Preceding page blank

Boundary Conditions for T-Foils: root support condition, strut-foil connection

Flutter Condition: U_f, f_f, mode shape

Nondimensional Flutter Parameter Ratios for Subcavitating T-Foils

Strut Parameters: L/c, AR (to root), κ, x_{ea} (y)/c, x_{cg} (y)/c, $4m$ (y)/$\pi\rho c^2$,

$\dfrac{16\,I_{my}(y)}{\pi\rho c^4}$, m_N (η), x_{eaN} (η), x_{cgN} (η), EI_N (η), GJ_N (η)

Pod Parameters: fineness ratio, (maximum diameter)/c, x_{nose}/c, x_{cg}/c,

M_{pod}/M_{strut}, $I_{y,pod}/I_{y,strut}$, $I_{\phi,pod}/I_{y,pod}$

Foil Parameters: c_{root}/c, AR, Λ, τ, x_{foil}/c, x_{ea} (z')/c, x_{cg} (z')/c, m_{foil} (3/4 span)/m_{strut}

(3/4 span), $I_{y,foil}/I_{y,strut}$, $I_{mz',foil}$ (3/4 span)/$I_{my,strut}$ (3/4 span),

$I_{\phi,foil}/I_{\phi,pod}$, EI_{foil} (3/4 span)/EI_{strut} (3/4 span), GJ_{foil} (3/4 span)/

GJ_{strut} (3/4 span), m_N (ζ'), $I_{mz'N}$ (ζ'), EI_N (ζ'), GJ_N (ζ')

System Parameters: ζ_s, μ (see text for approximate forms)

Nondimensional Boundary Conditions

Flutter Parameters: AR (wetted area), k_{nf}, $\dfrac{4\,EI\,(3/4\,span)}{\pi\rho c^2\,\omega_f^2\,L^4}$, $\dfrac{16\,GJ\,(3/4\,span)}{\pi\rho L^2\,\omega_f^2\,c^4}$,
normalized mode shape

These parameters were obtained from a modified strip theory that has been used in a large number of hydrofoil flutter calculations.[1,12,21] Some reduction was possible in the number of nondimensional parameters because several dimensioned parameters (L, c, Λ, E, I, G, J) appear only in combination with other parameters.

Two additional dimensionless ratios, Reynolds number R_n and Froude number F_n, are theoretically operative in flutter scaling. These parameters can usually be neglected for the following reasons. Flutter of both model and prototype usually occurs at relatively high speeds for which R_n is well above 4×10^5, the value above which changes in R_n have little effect on oscillatory loading on airfoils (see page 710 in Bisplinghoff et al.[6]) and should similarly not influence hydrofoil loading characteristics. It is therefore assumed that R_n can be neglected for hydrofoil flutter.

68

The effect of Froude number on hydrofoil loading has been studied for two-dimensional flow by Ashley et al.[39] They predict that as a result of interaction between the foil and the free surface, there will be a strong dependence on F_n when the foil is close to the surface and foil speed and oscillation frequency are low. It is expected that this interaction will be weaker in the three-dimensional case. Since hydrofoil systems will rarely if ever flutter at sufficiently low speeds and frequencies, Froude number is not important as a flutter parameter in the present case (subcavitating flow). It is shown below, however, that Froude number is necessarily preserved when naturally ventilated systems are scaled. Neither R_n nor F_n is required for scaling subcavitating flutter, but both parameters are included for reference in experimental results given in this report.

SUBCAVITATING DIVERGENCE

The parameters used to describe divergence are those flutter parameters which do not involve oscillation or inertia of the structure. EI and GJ are nondimensionalized in the form that would appear in the equations of motion of the structure.

Dimensioned Divergence Parameters for Subcavitating T-Foils

Strut Parameters: L, c, L cos Λ, x_{ea} (y), EI (y), GJ (y), ℓ

Pod Parameters: length, maximum diameter, x_{nose}

Foil Parameters: L, c (z'), L cos Λ, x_{foil}, x_{ea} (z'), EI (z'), GJ (z')

System Parameter: ρ

Boundary Conditions for T-Foils: root support condition, strut-foil connection

Divergence Condition: U_D, mode shape

---

[39]Ashley, H. et al., "New Directions in Lifting Surface Theory," AIAA Journal, Vol. 3, No. 1, pp. 3–16 (Jan 1965).

Strut Parameters: L/c, AR (to root), κ, x_{ea} $(y)/c$, EI_N (η), GJ_N (η)

Pod Parameters: fineness ratio, (maximum diameter)$/c$, x_{nose}/c

Foil Parameters: c_{root}/c, AR, Λ, τ, x_{foil}/c, x_{ea} $(z')/c$, EI_{foil} (3/4 span)$/$

EI_{strut} (3/4 span), GJ_{foil} (3/4 span)$/GJ_{strut}$ (3/4 span),

EI_N (z'), GJ_N (z')

Nondimensional Boundary Conditions

Divergence Parameters: AR (wetted area), $\dfrac{EI \ (3/4 \ span)}{2 \ \pi\rho \ U_D^{\,2} \ L^4}$, $\dfrac{2 \ GJ \ (3/4 \ span)}{\pi\rho \ U_D^{\,2} \ c^2 \ L^2}$,

normalized mode shape

FLUTTER OF CAVITATING AND VENTILATED SYSTEMS

Scaling flutter boundaries for cavitating and ventilated systems requires that hydrodynamic forces due to the cavitating or ventilated flow be similar in model and prototype systems. This will occur for similar profiles when cavitation number σ_c is equal at all equivalent depths in both systems where there is cavitation or ventilation. This may be expressed as

$$\sigma_c = \left.\frac{p_a + \rho gh - p_c}{\frac{1}{2} \ \rho \ U^2}\right|_{prototype} = \left.\frac{p_a + \rho gh - p_c}{\frac{1}{2} \ \rho \ U^2}\right|_{model}$$

or, in terms of velocity,

$$\frac{U^2_{\ prototype}}{U^2_{\ model}} = \frac{\rho_{model}}{\rho_{prototype}} \ \frac{(p_a + \rho gh - p_c)_{prototype}}{(p_a + \rho gh - p_c)_{model}}$$

The value of p_c varies according to the type of cavitation present. For natural ventilation, the expression is greatly simplified because, by definition, $p_c = p_a$. In that case, Froude number F_n is also preserved between the two systems. In general, however, preservation of F_n in addition to σ_c would place impractical requirements on p_a and p_c and would not be necessary so long as F_n is reasonably large (near 5.0).

70

It is noted for reference that few test facilities are capable of simulating cavitation conditions that occur for full-scale prototype operation above 50 knots. Flutter models of high-speed prototypes would generally have to be tested on the 150-knot carriage in the High-Speed Hydrodynamics Facility at Langley Field, Virginia[40] or, if a free surface is not required, in the 36-inch variable-pressure water tunnel[21] at NSRDC Carderock.

The requirement that σ_c be preserved between model and prototype fixes the values of stiffnesses El and GJ that must be used in a model. These values vary according to the type of cavitation present. The scaling laws for each type of cavitation are given in the section of this report dealing with known parameter trends of cavitating systems. Individual system parameters are listed below.

Dimensioned Flutter Parameters for Cavitating T-Foils

These include p_a, p_c, and surface geometry for all submerged components, in addition to all dimensioned flutter parameters previously given for subcavitating T-foils.

Nondimensional Flutter Parameter Ratios for Cavitating T-Foils

These include σ_c and nondimensionalized profiles for all submerged components, in addition to all nondimensional flutter parameters previously given for subcavitating T-foils.

DIVERGENCE OF SUBCAVITATING T-FOILS

Divergence parameters are the same as flutter parameters except for the removal of quantities involving structural inertia and oscillation frequency. The parameters given below were obtained from unpublished modified strip theory divergence equations.

---

[40]Olson, R.E. and W.F. Brownell, "Facilities and Research Capabilities–High Speed Phenomena Division. David Taylor Model Basin, Langley Field, Virginia," David Taylor Model Basin Report 1809 (Apr 1964).

**Dimensioned Divergence Parameters for
Subcavitating T-Foils**

Strut Parameters: L, c, L cos Λ, x_{ea} (y), EI (y), GJ (y), ℓ

Pod Parameters: length, maximum diameter, x_{nose}

Foil Parameters: L, c (z'), L cos Λ, x_{foil}, x_{ea} (z'), EI (z'), GJ (z')

System Parameter: ρ

Boundary Conditions for T-Foils: root support condition, strut-foil connection

Divergence Condition: U_D, mode shape

**Nondimensional Divergence Parameters for
Subcavitating T-Foils**

Strut Parameters: L/c, AR (to root), κ, x_{ea} (y)/c, EI_N (η), GJ_N (η)

Pod Parameters: fineness ratio, (maximum diameter)/c, x_{nose}/c

Foil Parameters: κ, AR, x_{foil}/c, x_{ea} (z')/c, EI_N (ζ'), GJ_N (ζ')

Nondimensional Boundary Conditions

Divergence Condition: AR (wetted area), $\dfrac{EI \ (3/4 \ \text{span})}{2 \ \pi\rho \ L^4 \ U_D^2 \ \cos^2 \Lambda}$, $\dfrac{2 \ GJ \ (3/4 \ \text{span})}{\pi\rho \ c^2 \ L^2 \ U_D^2 \ \cos^2 \Lambda}$,

normalized mode shape

DIVERGENCE OF CAVITATING AND VENTILATED T-FOILS

**Dimensioned Divergence Parameters for
Cavitating T-Foils**

These include p_a, p_c, surface geometry for all submerged components, in addition to all dimensioned divergence parameters previously given for subcavitating T-foils.

**Nondimensional Divergence Parameter Ratios
for Cavitating T-Foils**

These include σ_c and nondimensionalized profiles for all submerged components, in addition to all nondimensional divergence parameters previously given for subcavitating T-foils.

REFERENCES

1. Besch, P.K. and Y.-N. Liu, "Bending Flutter and Torsional Flutter of Flexible Hydrofoil Struts," Ninth Symposium on Naval Hydrodynamics, Paris, France (Aug 1972); also NSRDC Report 4012 (Feb 1973).

2. Mitchell, L. and F.J. Rauch, Jr., "Dynamic Tests of the 1/4-Scale Models of the 80-Knot Transiting Strut-Foil Systems for the FRESH I Hydrofoil Test Craft," Grumman Aircraft Engineenng Corporation, Contract NObs 86826 (Aug 1964).

3. Kennard, E.H., "Irrotational Flow of Frictionless Fluids, Mostly of Invariable Density," David Taylor Model Basin Report 2299, pp. 390–392 (Feb 1967).

4. Scanlan, R.H. and R. Rosenbaum, "Aircraft Vibration and Flutter," Dover Publications, Inc., New York (1968).

5. Schaffer, A.P., "Flutter Flight Testing of a High Speed Hydrofoil Craft–The H.S. DENISON," Grumman Aircraft Engineering Corporation Report FT-HYD-Ia.1 (Apr 1963).

6. Bisplinghoff, R.T. et al., "Aeroelasticity," Addison-Wesley Publishing Company, Inc., Cambridge, Massachusetts (1955).

7. Hilborne, D.V., "The Hydroelastic Stability of Struts," Admiralty Research Laboratory (Great Britain) Report ARL/R1/G/HY/5/3 (1958).

8. Huang, T.T., "Experimental Study of a Low Modulus Flutter Model for Strut-Foil-Pod Configurations," Hydronautics, Inc. Technical Report 459-2 (Jul 1967).

9. Squires, C.E., Jr., "Hydrofoil Flutter, Small Sweep Angle Investigation–Final Report," Grumman Aircraft Engineering Corporation Report DA Nonr-3989.3 (Nov 1963).

10. Baird, E.F. et al., "Investigation of Hydrofoil Flutter–Final Report," Grumman Aircraft Engineering Corporation Report DA 10-480-3 (Feb 1962).

11. Abramson, H.N. and G.E. Ransleben, Jr., "An Experimental Investigation of Flutter of a Fully Submerged Subcavitating Hydrofoil," J. Aircraft, Vol. 2, No. 5, pp. 439–442 (Sep–Oct 1965).

12. Besch, P.K. and Liu, Y.-N., "Flutter and Divergence Characteristics of Four Low Mass Ratio Hydrofoils," NSRDC Report 3410 (Jan 1971).

13. Woolston, D.S. and G.E. Castile, "Some Effects of Variations in Several Parameters Including Fluid Density on the Flutter Speed of Light Uniform Cantilever Wings," NACA TN 2558 (1951).

14. Ransleben, G.E., Jr., "Experimental Determination of Variation of Hydrofoil Flutter Speed with Mass Ratio," Southwest Research Institute, Contract N00014-69-C-0219 (Apr 1970).

15. Ransleben, G.E., Jr., "Description of a One-Eighth Scale Flutter Model of the Main Hydrofoil Assembly of the AG(EH) 800 Hydrofoil Research Ship," Southwest Research Institute Project 02-1960 (Dec 1966).

16. Peoples, J.R., "Frequencies and Damping of Full Scale Hydrofoils by "Pluck Test" Methods," 43rd Shock and Vibration Bulletin, Shock and Vibration Information Center, Naval Research Laboratory (Jun 1973).

17. "PCH-1 Mod 1 Detail Design—Structural Summary," The Boeing Company (1969).

18. Brownell, W.F. and M.L. Miller, "Hydromechanics Cavitation Research Facilities and Techniques in Use at the David Taylor Model Basin," Symposium on Cavitation Research Facilities and Techniques, American Society of Mechanical Engineers (May 1964); also David Taylor Model Basin Report 1856 (Oct 1964).

19. White, R.G., "Use of Transient Excitation in the Dynamic Analysis of Structures," The Aeronautical Journal of the Royal Aeronautical Society, Vol. 73, pp. 1047–1050 (Dec 1969).

20. Yates, E.C., Jr., "Flutter Prediction at Low Mass-Density Ratios with Application to the Finite-Span Noncavitating Hydrofoil," American Institute of Aeronautics and Astronautics Third Marine Systems and ASW Meeting (Apr–May 1968).

21. Liu, Y.-N. and P.K. Besch, "Hydrofoil Flutter Analysis, Using a Modified Strip Theory," NSRDC Report 3624 (Jul 1971).

22. Rowe, W.S. and T.G.B. Marvin, "A Program of Theoretical Research on Hydroelastic Stability," The Boeing Company, Contract N00014-67-C-0248 (Nov 1968).

23. Clark, D.J., "Instrumentation and Static Calibration of the Foil Systems of the Navy Hydrofoil Boat PLAINVIEW (AG(EH)-1)," David Taylor Model Basin Report 2149 (Jan 1966).

24. "AGEH-1 Weight Control Report—Final," Lockheed Shipbuilding and Construction Company (Jul 1969).

25. Ransleben, G.E., Jr. and P.A. Cox, Jr., "Comparison of Measured Natural Frequencies of the One-Eighth Scale AG(EH) Flutter Model with Calculated Full-Scale Frequencies," Southwest Research Institute Project 02-2260, Contract N00600-68-D-0375 (Mar 1968).

26. Abramson, H.N. et al., "Hydroelasticity with Special Reference to Hydrofoil Craft," NSRDC Report 2557 (Sep 1967).

27. French, H., "Hydrofoil Patrol Craft PC(H) Fwd Hydrofoil Vibration Modes," The Boeing Company, Aerospace Division, Bureau of Ships Plan PC(H) – 1 518 1993317 (Oct 1961).

28. Caspar, J.R., "Divergence Analysis of Swept Hydrofoils--Computer Program (SWDIVRG)," NSRDC Report 4245 (Apr 1974).

29. Peterson, L., "Theoretical Basis for SADSAM Computer Program," MacNeal-Schwendler Corporation Project Report (Dec 1970).

30. Besch, P.K., "Flutter and Cavity-Induced Oscillation of a Two-Degree-of-Freedom Hydrofoil in Two Dimensional Cavitating Flow," NSRDC Report 3000 (Apr 1969).

31. Cieslowski, D.S. and P.K. Besch, "Flutter of a Two-Degree-of-Freedom Hydrofoil in Two-Dimensional Subcavitating Flow," NSRDC Report 3183 (Jan 1970).

32. Song, C.S., "Flutter of Supercavitating Hydrofoils–Comparison of Theory and Experiment," Journal of Ship Research, Vol. 16, No. 3, pp. 153–166 (Sep 1972).

33. Squires, C.E., Jr., "Preliminary Flutter Analysis of the Design M-51 Hydrofoil Craft (FRESH I)," Grumman Aircraft Engineering Corporation Report DA M51-478.i (Mar 1963).

34. Steinberg, H. and S. Karp, "Unsteady Flow Past Partially Cavitated Hydrofoils," Proceedings Fourth Naval Hydrodynamics Symposium (Aug 1962).

35. Kaplan, P. and C.J. Henry, "A Study of the Hydroelastic Instabilities of Super-cavitating Hydrofoils," Journal of Ship Research, Vol. 4, No. 3, pp. 28–38 (Dec 1960).

36. Ransleben, G.E., Jr., "Experimental Determination of Steady and Unsteady Loads on a Surface Piercing, Ventilated Hydrofoil," Journal of Ship Research, Vol. 13, No. 1, pp. 1–11 (Mar 1969).

37. Langhaar, H.L., "Dimensional Analysis and Theory of Models," John Wiley & Sons, Inc., New York (1951).

38. Albertson, M.L. et al., "Fluid Mechanics for Engineers," Prentice-Hall, Inc., Englewood Cliffs, N.J. (1960).

39. Ashley, H. et al., "New Directions in Lifting Surface Theory," AIAA Journal, Vol. 3, No. 1, pp. 3–16 (Jan 1965).

40. Olson, R.E. and W.F. Brownell, "Facilities and Research Capabilities–High Speed Phenomena Division, David Taylor Model Basin, Langley Field, Virginia," David Taylor Model Basin Report 1809 (Apr 1964).